https://doi.org/10.5194/nhess-2024-76
Preprint. Discussion started: 22 May 2024

Natural Hazards and Earth System Sciences
Discussions

Predicting the thickness of shallow landslides in Switzerland using machine learning

Christoph Schaller[1,2], Luuk Dorren[1], Massimiliano Schwarz[1], Christine Moos[1], Arie C. Seijmonsbergen[2], and E. Emiel van Loon[2]

[1]Bern University of Applied Sciences - HAFL, Länggasse 85, 3052 Zollikofen, Switzerland
[2]University of Amsterdam UVA - IBED, Sciencepark 904, 1098 XH Amsterdam, The Netherlands

Correspondence: Christoph Schaller (christoph.schaller@bfh.ch)

Abstract. Landslide thickness is a key parameter in various types of models used to simulate landslide susceptibility. In this study, we developed a model providing improved predictions of potential shallow landslide thickness in Switzerland. We tested three machine learning models based on random forests, generalized additive model, and linear regression and compared the results to three existing models that link soil thickness to slope and elevation. The models were calibrated using data from two field inventories in Switzerland ("HMDB" with 709 records and "KtBE" with 517 records). We explored 37 different covariates including metrics on terrain, geomorphology, vegetation height, and lithology at three different cell sizes. To train the machine learning models, 21 variables were chosen based on the variable importance derived from random forest models and expert judgement. Our results show that the machine learning models consistently outperformed the existing models by reducing the mean absolute error by at least 17%. The random forests models produced a mean absolute error of 0.25 m for the HMDB and 0.19 m for the KtBE data. Models based on machine learning substantially improve the prediction of landslide thickness, offering refined input for enhancing the performance of slope stability simulations.

1 Introduction

Rainfall-induced landslides pose serious threats to infrastructure and inhabited areas worldwide (Froude and Petley, 2018; Emberson et al., 2020). In Switzerland, such spontaneous landslides regularly cause extensive infrastructure damage and closures, evacuations and even fatalities. By way of example, 74 people died as a result of 40 different landslide events between 1946 and 2015 (Badoux et al., 2016). During a rainfall event in August 2005, shallow landslides (definition provided below) and the resulting hillslope debris flows caused damage amounting to CHF 150 million across Switzerland within 48 hours (Bezzola and Hegg, 2007). Approximately CHF 15 million are spent each year on landslide protective measures in Switzerland (Dorren et al., 2009). To mitigate this risk, regional landslide hazard mapping and modelling provide an important basis for indicating potential hazard areas (Dahl et al., 2010; Kaur et al., 2019; Shano et al., 2020; Di Napoli et al., 2021). In Switzerland, national-scale shallow landslide modelling was carried out at within the SilvaProtect-CH project (Dorren and Schwarz, 2016). Results from this project have provided an important basis for different stakeholders and policymakers, e.g., for the delimitation of

https://doi.org/10.5194/nhess-2024-76
Preprint. Discussion started: 22 May 2024


Natural Hazards and Earth System Sciences
Discussions

landslide protection forest areas across the country and the preliminary risk analyses for national roads (Arnold and Dorren, 2015) and railways.

In general, landslides can be defined as the movement of a rock or soil mass along a slope (Varnes, 1978; Hungr et al., 2014). The term "shallow landslides" typically refers to translational sliding movements of soil material (earth and/or debris) from the upper soil layers, characterized by a well-defined sliding surface (Cruden and Varnes, 1996; Hungr et al., 2014). Often, shallow landslides result in hillslope debris flows, which, because of their velocity and resulting impact pressure, can be very destructive (Zimmermann et al., 2020). Landslides are usually classified as shallow landslides if the thickness of the instable mass does not exceed 2 m (which is also used as a definition in Switzerland, (Lateltin et al., 2005)), although in some cases, this limit lies at 3 meters (Sidle and Ochiai, 2013; Rickli et al., 2019; Li and Mo, 2019). With a median release area of around 200 m^2 and an average thickness of 0.5 m to 1 m, shallow landslides generally fall into the category of small (10^0–10^3 m^3) and occasionally into the category of very small (10^{-3}–10^0 m^3) or medium (10^3–10^6 m^3) landslides as proposed by McColl and Cook (2024). In this study, we define landslide thickness as the average thickness of the instable mass, measured from, and perpendicularly to, the original slope surface to the failure plane (see T_L in Fig. 1).

Landslide thickness is a key parameter in various types of models for simulating landslide susceptibility. These models can be grouped into three categories: conceptual models, empirical models (data-driven models, e.g., statistical, machine learning), and physically-based models (Murgia et al., 2022). Conceptual models aim to provide a simplified methodology for estimating changes in slope stability (Murgia et al., 2022) e.g. using cellular automaton models (Piegari et al., 2006). The physically-based models can be further divided into deterministic (e.g., Montgomery and Dietrich, 1994; Baum et al., 2002) and probabilistic models (e.g., Pack et al., 1998; Horton et al., 2013; van Zadelhoff et al., 2022). Empirical models predict landslide occurrence based on factors that can be directly or indirectly linked to slope instability (Reichenbach et al., 2018). Such models are gaining interest due to improved data availability/quality and increasing research on machine learning and other computational techniques (Merghadi et al., 2020). Various studies have shown that the accuracy of the potential landslide thickness is of paramount importance for the performance of slope stability models (cf. Iida, 1999; Larsen et al., 2010; Milledge et al., 2014). This is also confirmed by our recent paper on the SlideForMAP (SFM) model for spatially distributed regional assessment of shallow landslide susceptibility van Zadelhoff et al. (2022)). Consequently, improving the estimation of landslide thickness is key for enhancing the performance of slope stability models. With the overall aim of developing a model that provides a more accurate prediction of the potential landslide thickness compared to existing models, the four main objectives of this study are:

- to present descriptive statistics on data on the thickness of shallow landslides and additional potentially explanatory data from three field inventories in Switzerland,
- to develop and test models for predicting the potential thickness of shallow landslides in Switzerland based on machine learning (random forests (RF), generalized additive models (GAM), and linear regression (LM)) using input variables including terrain metrics and vegetation height,
- to evaluate the performance of the developed models using data from the two landslide inventories,

https://doi.org/10.5194/nhess-2024-76
Preprint. Discussion started: 22 May 2024


Natural Hazards and Earth System Sciences
Discussions

– to compare the performance of the developed models with three previously published methods that predict landslide thickness based on altitude, slope, and cumulative slope distribution.

2 Theoretical background

2.1 Influences on landslide failure thickness

The mechanisms for inducing shallow landslides depend on geological formations, landscapes, and soil types (Hungr et al., 2014; Watakabe and Matsushi, 2019; Chinkulkijniwat et al., 2019). Most landslides occur in wet, partially saturated soils due to prolonged or intense rainfall, snowmelt, or seismic activity (Leonarduzzi et al., 2017; Schuster and Wieczorek, 2018). An increasing water content in the soil induces a reduction of soil shear strength leading to the failure of soil material within a shear band, usually situated at the interface of below-ground discontinuities such as between soil and bedrock (Catani et al., 2010; Zhang et al., 2017; Xiao et al., 2023) or between different soil horizons (Li et al., 2013; Ali et al., 2014; Ran et al., 2018; Chinkulkijniwat et al., 2019). This boundary defines the failure plane of shallow landslides and is as such implemented in physically-based models (Ran et al., 2018). The hydrological properties of the soil and the local hydrological conditions (such as the rainfall characteristics and the runoff disposition of the upslope area, as well as the groundwater table and the pore-water pressure) influence the occurrence and depth of failure plane of shallow landslides (Caine, 1980; Iverson, 2000; Guzzetti et al., 2008b; Li et al., 2013; Chinkulkijniwat et al., 2019).

In many studies, soil thickness is used as a proxy for landslide thickness (e.g., Montgomery and Dietrich, 1994; Pack et al., 1998; Iida, 1999; Baum et al., 2002; D'Odorico and Fagherazzi, 2003; Segoni et al., 2012; Ho et al., 2012; Merghadi et al., 2020). When describing or modelling landslides, care should be taken to define the thickness unambiguously. Sometimes the terms soil thickness and depth are used interchangeably. However, in most studies, depth refers to a measurement in the vertical direction, while thickness refers to a measurement perpendicular to the slope of the local surface (e.g., Meisina and Scarabelli, 2007; Catani et al., 2010; Jia et al., 2012; Ho et al., 2012; Lanni et al., 2012; Patton et al., 2018). Some studies use a reverse definition of the two terms (e.g., Cruden and Varnes, 1996; Pack et al., 1998). Similarly, the depth of the failure plane may be defined in the vertical direction (Watakabe and Matsushi, 2019; Meier et al., 2020; Chang et al., 2021) or perpendicular to the slope (Iida, 1999; Schwarz et al., 2010; Li et al., 2013). The perpendicular direction seems to be favoured if the values are also used for volume calculations (WSL and BAFU, 2018; Jaboyedoff et al., 2020; Hählen, 2023). In this study, we use the term depth when measuring in the vertical direction (see depth at scarp D_F and soil depth D_S in Fig. 1) and thickness when measuring perpendicular to the slope (T_L in Fig. 1).

https://doi.org/10.5194/nhess-2024-76
Preprint. Discussion started: 22 May 2024

Natural Hazards and Earth System Sciences
Discussions

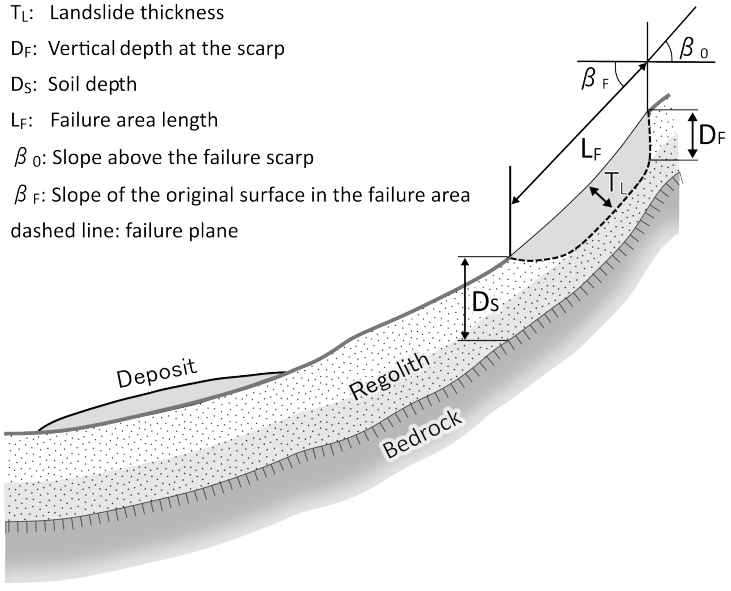

Figure 1. Schematic representation of a shallow landslide with its failure area, transit zone and deposit, including important definitions used in this study.

2.2 Models for estimating soil thickness for landslide modelling

The landslide thickness values used for shallow landslides assessment are usually based on field measurements (e.g., by digging soil pits (Catani et al., 2010) or by drilling (Xiao et al., 2023)) or on data from landslide inventories (van Zadelhoff et al., 2022). However, dense field measurements are only available for small extents and even then, the resulting soil thickness maps have high uncertainties due to the large heterogeneity of soil parameters (Cohen et al., 2009; Jia et al., 2012; Lanni et al., 2012). To deal with the uncertainties in landslide thickness, different modelling approaches have been adopted. Table 1 gives a non-exhaustive overview of such models found in literature. Most of these models are either deterministic (e.g., Montgomery and Dietrich, 1994; Baum et al., 2002) or probabilistic (e.g., Pack et al., 1998; Horton et al., 2013; van Zadelhoff et al., 2022). In addition, the use of machine learning methods to predict inputs for landslide models including soil thickness is also becoming more commonplace (Hengl et al., 2017; Merghadi et al., 2020; Wadoux et al., 2020; Xiao et al., 2023).

https://doi.org/10.5194/nhess-2024-76
Preprint. Discussion started: 22 May 2024

Natural Hazards and Earth System Sciences Discussions

Table 1. Non-exhaustive list with a summary of soil thickness models found in literature.

Model used	Parameters	Relationship with soil depth	Reference
Constant soil thickness across the study area	Mean soil thickness, possibly combined with standard deviation	Constant value	Montgomery and Dietrich (1994); Baum et al. (2002); Ho et al. (2012)
Elevation	elevation	Linear scaling	Saulnier et al. (1997); Catani et al. (2010); Segoni et al. (2012)
Slope gradient linear	slope gradient	Linear scaling	Saulnier et al. (1997); Catani et al. (2010); Segoni et al. (2012)
		Linear relationship statistically fitted	Lanni et al. (2012)
Slope gradient exponential	slope gradient	Exponential law	(Segoni et al., 2012)
Slope gradient cumulative	thickness measurements and slope values from a landslide inventory	Cumulative normal distribution of slope values	van Zadelhoff et al. (2022)
Hillslope curvature	Curvature	Linear relationship; varies across different landscapes as a function of the standard deviation in catchment curvatures	Patton et al. (2018)
Topographic Wetness Index (TWI)	TWI	Linear relationship	Ho et al. (2012)
Linear model with terrain indices	slope gradient, plan curvature, profile curvature, specific catchment area, and relative position on the hillslope	Linear relationship established by multi-linear regression	Jia et al. (2012)
Process-based models	time since last denuding by landslides	linked to soil development over time by approximating the development using a logarithmic function	Iida (1999)
	bulk density of the rock, elevation, slope	mass balance between soil production from underlying bedrock and the divergence of diffusive soil transport by solving the evolving soil depth using a finite difference model under varying initial conditions	Dietrich et al. (1995)
GIST (Geomorphologically Indexed Soil Thickness)	slope gradient, horizontal and vertical slope curvature, relative position within the hillslope profile	the gradient and curvature are connected to the kinematic stability of the regolith cover while the distance from the hill crest accounts for the position within the soil toposequence	Catani et al. (2010); Segoni et al. (2012); Xiao et al. (2023)
sGIST	slope gradient, horizontal and vertical slope curvature, relative position within the hillslope profile	GIST without geomorphological indexing	Catani et al. (2010); Segoni et al. (2012)
GIST-RF	GIST inputs plus altitude, plan curvature, and Terrain Roughness Index (TRI) as covariates	Random forests regression	Xiao et al. (2023)
Machine learning ensemble	158 remote sensing-based covariates	ensemble including random forests and gradient boosting and/or multinomial logistic regression	Hengl et al. (2017)

3 Materials

3.1 Landslide inventories

This study used datasets based on three different landslide inventories in Switzerland as reference data. Since the data also includes landslides with medium and deep thickness, only entries with a thickness of up to 2.5 m were retained for this study.

The first dataset (hereafter "HMDB") is based on a comprehensive database of shallow landslides and hillslope debris flows created by Rickli et al. (2016, 2019), an inventory containing shallow landslides in Switzerland that occurred between 1997 and 2021. The data in this inventory is based on field surveys performed with analogue protocols that include relevant parameters

https://doi.org/10.5194/nhess-2024-76
Preprint. Discussion started: 22 May 2024


Natural Hazards and Earth System Sciences
Discussions

such as the dimensions of the landslides, site characteristics, and runout characteristics (Rickli and Graf, 2009; WSL and BAFU, 2018). If values could not be measured in the field (e.g., because of terrain changes since the event), the database may contain estimated values that are marked accordingly (Rickli et al., 2016). Of 760 entries in the inventory, 711 comprised either measured or estimated thickness values perpendicular to the original slope surface (see T_L in Fig. 1). Of these 711, 75 records had measured thickness values and 199 records had estimated thickness values already present in the database. The values for the remaining 435 records were estimated by dividing the landslide volume by the failure area. This approach was chosen since the mean landslide thickness in the HMDB is mainly used for the estimation of the failure volume (Rickli et al., 2016; Rickli, 2023). Two records with an estimated value larger than 2.5 m were removed, leaving 709 records actually used in the filtered dataset.

The second dataset (hereafter "KtBE") is based on an inventory created by the office for natural hazards of the canton of Bern Hählen (2023) and comprises 519 landslides, 6 of which are also recorded in the HMDB inventory. The landslides in the KtBE inventory were recorded between 2005 and 2021. For the inventory, the failure zones and runout envelopes of shallow landslides were digitized from orthophotos. The runout volume and mean thickness of the landslides were estimated by expert opinion from the orthophotos. The author estimated an error of between 25% to 50% for the thickness (Hählen, 2023). Since only events the entire process area of which could be reliably reconstructed from the orthophotos were recorded, many events in forests or intensively cultivated areas were not included in the inventory. This limits the possibility of making comparisons between landslides within and outside of forests, as well as the possibility of making statements about the local occurrence frequency of landslides based on the data. From the 519 entries, two were excluded from the final dataset because of a missing thickness value and a thickness value larger than 2.5 m.

The third dataset (hereafter "StorMe"), comprising 5733 records on shallow landslides, was derived from an export of the Swiss national register of natural hazard events that is maintained by the Federal Office for Environment (FOEN) and the cantons (Burren and Eyer, 2000). This dataset was only used for descriptive statistics and was excluded from model development due to problems with the data quality. While there is a manual for the data collection for this register (Bühlmann and Ruf, 2020), the records are not only missing a large number of values but also contain numerous unrealistic values, which can be attributed to rough estimates by many different experts performing the surveys. Therefore, we included only landslides with a thickness of less than or equal to 2.5 m that were reportedly measured in the field, thus excluding almost half of the exported landslide entries in the register and leaving 2988 records in the dataset. Figure 2 shows the distribution of the landslides per dataset across Switzerland. Table 2 lists the number of landslides per canton and inventory. The fact that the datasets only contain records for 14 of the 26 cantons in Switzerland is not only caused by uneven occurrence of landslides but also by differences in the availability of recorded data. While the recorded landslides are distributed across large parts of Switzerland, there is a clear concentration on the northern parts of the Alps and Pre-Alps. The landslides in the HMDB dataset are concentrated in the cantons Obwalden, Bern, Grisons, Appenzell, Lucerne, Vaud, and Zurich. These entries show local clusters that mostly were caused by specific extreme precipitation events in combination with unfavourable geological undergrounds such as flysch or molasse (Reynard et al., 2021; Steger et al., 2022). Most of the landslides of the KtBE dataset lie in the canton of Bern, while a few landslides are across the borders in the cantons of Fribourg and Lucerne. Most of the

https://doi.org/10.5194/nhess-2024-76
Preprint. Discussion started: 22 May 2024


Natural Hazards and Earth System Sciences
Discussions

135 landslides in the StorMe inventory are recorded for the cantons of Bern, Grisons, and Obwalden with lower counts for the other cantons.

Table 2. Number of recorded landslides per canton in the datasets

Canton	HMDB	KtBE	StorMe
Appenzell Ausserrhoden	103	0	12
Appenzell Innerrhoden	2	0	0
Bern	170	483	1980
Fribourg	0	1	14
Grisons	106	0	410
Lucerne	86	33	97
Nidwalden	0	0	53
Obwalden	240	0	232
Schwyz	0	0	60
Solothurn	0	0	29
Uri	0	0	72
Vaud	1	0	0
Zug	0	0	29
Zürich	1	0	0
Total	709	517	2988

https://doi.org/10.5194/nhess-2024-76
Preprint. Discussion started: 22 May 2024

Natural Hazards and Earth System Sciences
Discussions

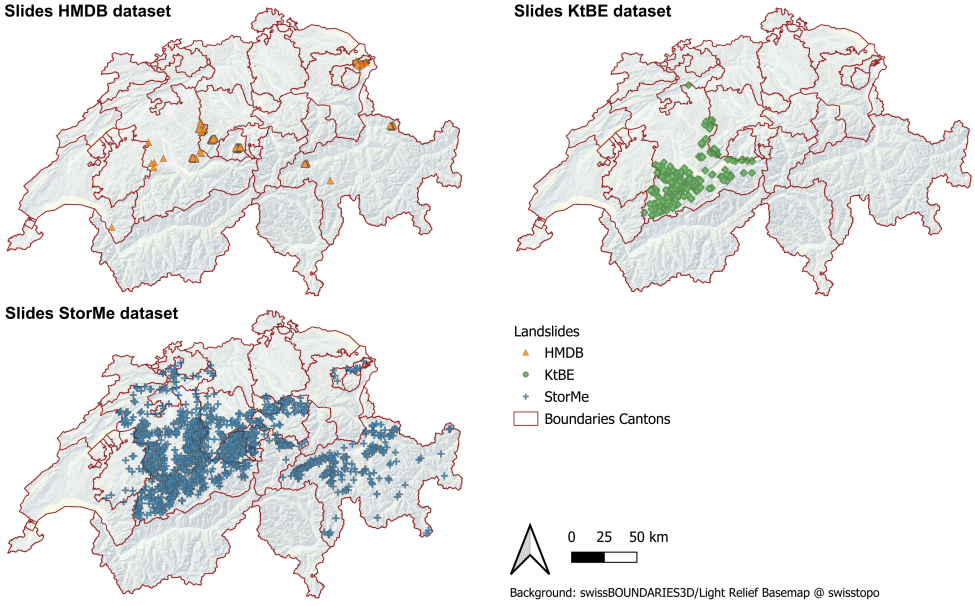

Figure 2. Map showing the locations of the observed shallow landslides across Switzerland for the HMDB (orange triangles), KtBE (green diamonds), and StorMe (blue cross) datasets.

3.2 Model input data

The following datasets are used as input for calculating the covariates for the modelling in this study:

- The LiDAR (Light Detection And Ranging)-based swissALTI3D digital elevation model (DEM) with 0.5 m cell size (Swisstopo, 2023a) was used as the basis for the terrain analysis.
- Areas outside of the Swiss borders not covered by swissALTI3D were filled in using the 25 cell size EU-DEM v1.1 (EEA, 2016) to prevent missing data within the areas analysed.
- A LiDAR-based vegetation height model (VHM) with 1 m cell size (c.f. Schaller et al., 2023) was used as input for calculating statistics on vegetation height.
- Modelled data on extreme point precipitation (Frei and Fukutome, 2022) with 1 km cell size for different return periods (2, 10 30, 50, 100, 200, and 300 years). This input was used as a proxy variable indicating locations with possibly extreme rainfall amounts associated with increased landsliding activity, assuming that this leads to less soil cover.
- To represent the underlying geology, the vector-based dataset representing the rock densities across Switzerland was used (Swisstopo, 2020). The density of rocks varies based on their chemical composition and the structure of their minerals (from crystalline to amorphous) (Zappone and Kissling, 2021). Each entry in the dataset is assigned to one of the 21 defined lithological groups and it shows the expected range in which the mean bulk density of the local lithology varies (Swisstopo, 2020).

https://doi.org/10.5194/nhess-2024-76
Preprint. Discussion started: 22 May 2024


Natural Hazards and Earth System Sciences
Discussions

– The topographic catchments areas of Swiss water bodies (BAFU, 2019) served as a basis for tiling the input data for parallel processing of the covariate inputs.

4 Methods

The methodology applied in this study is divided into three stages (Fig. 3). In stage 1, intermediate DEM rasters for the subsequent stage were prepared. During stage 2, the data used for the final modelling and analysis stage were prepared. First, the covariates like terrain variables or geology were derived based on the DEM and other inputs. Then, the covariates were added to the reference data by sampling the generated rasters at the landslide failure points. The analysis and modelling based on the previously prepared dataset were performed in stage 4 including the training of three types of machine learning (ML) models and the application of three existing model types.

https://doi.org/10.5194/nhess-2024-76
Preprint. Discussion started: 22 May 2024

Natural Hazards and Earth System Sciences
Discussions

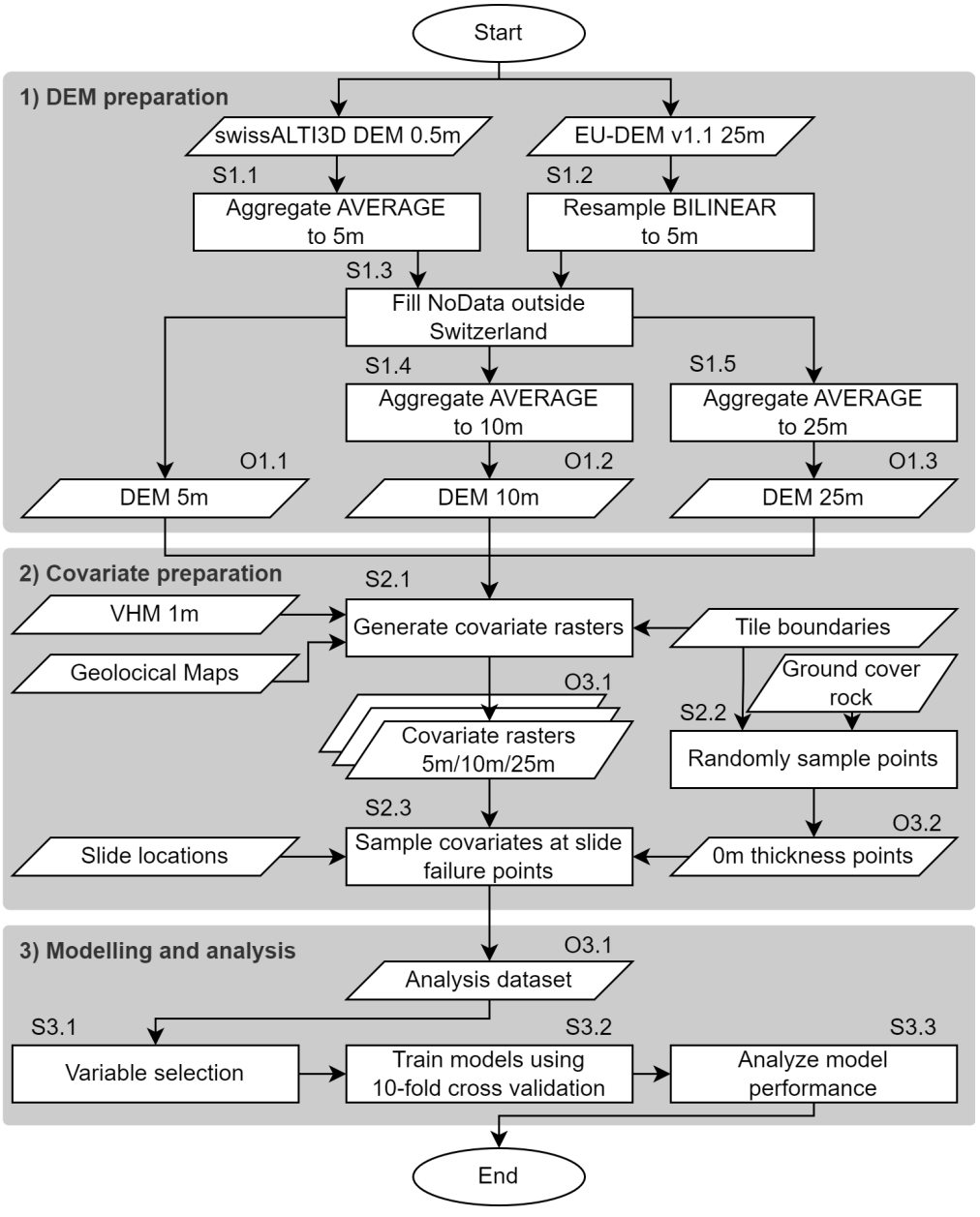

Figure 3. Flowchart of the methodology applied for this study. The three separate grey boxes delineate the 1) DEM preparation, 2) covariate preparation and 3) modelling and analysis stages. Square boxes denote process steps while parallelograms denote datasets.

All three stages were implemented in the R environment for statistical computing (Team, 2022). While the calculation of some variables was implemented in R using the sf (Pebesma and Bivand, 2023) and terra (Hijmans, 2023) packages, the processing of most variables was implemented using SAGA GIS (System for Automated Geoscientific Analyses, Conrad et al. (2015)) via the RSAGA package (Brenning, 2008) or using GDAL (Geospatial Data Abstraction Library) tools (GDAL/OGR

https://doi.org/10.5194/nhess-2024-76
Preprint. Discussion started: 22 May 2024


Natural Hazards and Earth System Sciences
Discussions

contributors, 2021) called from R. The code for the entire process can be found in the repository accompanying this study (Schaller, 2024).

4.1 DEM preparation

The covariates for the modelling step were calculated as rasters with a cell size of 5 m, 10 m, and 25 m (outputs O1.1, O1.2, and O1.3 in Fig. 3). The 0.5 m cell size swissALTI3D DEM was used as input for the terrain-based covariates. The original DEM was first aggregated to 5 m cell size using gdalwarp with the average function (step S1.1 in Fig. 3). Since some variables were calculated with large window sizes, the areas outside the Swiss borders not covered by swissALT3D were filled using the EU-DEM. For this purpose, the original extent of the 5 m DEM was first buffered by 4 km (step S1.2 in Fig. 3). The areas with NoData within that buffered extent were then filled using values from the EU-DEM resampled to 5 m using gdalwarp with a bilinear function (step S1.3 in Fig. 3). This filled raster was the primary input for the terrain analysis. The additional DEM rasters with 10 m and 25 m cell sizes were derived by aggregating the filled 5 m DEM using gdalwarp with the average function (steps S1.4 and S1.5 in Fig. 3).

4.2 Covariate preparation

4.2.1 Calculating covariate rasters

As stated in the previous section, the covariates for the modelling and analysis step were calculated as rasters with 5 m, 10 m, and 25 m cell sizes. Some covariates were calculated for all three cell sizes while others were only calculated for specific cell sizes. Table 3 gives an overview of the processed variables and their corresponding cell sizes. The terrain-based covariates calculated from the DEM included metrics commonly used in terrain analysis, hydrology, and geomorphology that were also used in other studies aiming to predict failure or soil depth. The covariates not based on the DEM include a variety of input data on ground cover, vegetation, geology, and precipitation. Vector-based input data was rasterized, including the generation of separate 0/1 encoded rasters for categorical variables.

To optimize the calculation of covariates for the entire area of Switzerland, the processing of the covariates was parallelized (step S2.1 in Fig. 3). For this purpose, Switzerland was divided into tiles based on aggregated catchments. The pre-defined aggregation level of the topographic watershed dataset (BAFU, 2019), which defines watersheds with a size of around 150 km^2, was used since they correspond to a tile size with acceptable processing times while keeping the number of tiles at a manageable level. For the actual processing, the extents of the catchments were by default buffered by 500 m to allow for overlap between the tiles and to accommodate window sizes that go beyond the catchment border. For the 25 m cell size DEM raster, however, the buffer was extended to 4 km, since some covariates use such a large window. Note that variables connected to hydrology were not calculated based on the original DEM raster, but a sink-filled version of the DEM that was generated using the SAGA GIS Tool "Fill Sinks" based on the method by Planchon and Darboux (2002).

https://doi.org/10.5194/nhess-2024-76
Preprint. Discussion started: 22 May 2024

Natural Hazards and Earth System Sciences
Discussions

Table 3. Variables explored as covariates for the machine learning models in this study.

	Cell size		
Name	**5 m**	**10 m**	**25 m**
Elevation above sea level	x[1]	x	x
Slope in degrees	x	x[1]	x
Aspect in degrees	x	x	x
Aspect northness	x	x[1]	x
Aspect eastness	x	x	x
Catchment area	x	x	x[1]
Catchment slope	x	x	x[1]
Modified catchment area	x	x	x
Topographic wetness index	x	x	x
Topographic wetness index SAGA	x[1]	x	x
Flow accumulation (top-down) contributing area	x	x	x
General curvature	x	x[1]	x
Profile curvature	x	x	x[1]
Plan curvature	x	x	x
Elevation percentile with 50 m and 200 m radius	x		
Negative openness with 50 m and 200 m radius	x[1]		
Topographic Position Indexes (TPI) for 15 m, 50 m, 200 m, 500 m, 1 km, 2 km, and 4 km	x	x	x[1]
Multiresolution Index of Valley Bottom Flatness (MRVBF)	x	x[1]	x
Multiresolution Index of the Ridge Top Flatness (MRRTF)	x	x	x[1]
Convergence index	x	x	x
Upslope curvature	x	x	x
Downslope curvature	x	x	x
Morphometric protection Index	x	x	x
Vector Ruggedness Measure (VRM)	x	x	x[1]
Terrain Ruggedness Index (TRI)	x[1]	x[1]	x
Slope height	x	x	x[1]
Valley depth	x	x	x[1]
Normalized height	x	x	x
Standardized height	x	x	x[1]
Mid-slope position	x	x	x
Toposcale	x	x	x
Geomorphon with 50 m and 200 m radius	x		
Groundcover swissTLM3D	x		
Extreme point precipitation values for 60 min duration with 10-year return period			x
Maximum and 75th percentile statistics of vegetation height within cell based on 1 m cell size VHM	x[1]	x	x
Mean density of the underlying rock	x[1]		

x[1] Variables and cell size used in the final ML-models.

4.2.2 Sampling covariate values

After calculating the covariate rasters, we prepared the dataset for the subsequent modelling and analysis stage. This was achieved by enriching the event data from the inventories with the covariate values by sampling the cell values at the failure

https://doi.org/10.5194/nhess-2024-76
Preprint. Discussion started: 22 May 2024


Natural Hazards and Earth System Sciences
Discussions

point of the landslides (step S2.3 in Fig. 3). In the case of the HMDB dataset, the reported coordinates of the failure point were directly used. For the KtBE dataset, only the event envelopes were available as input. Therefore, the failure point was approximated by taking the mean of the x and y coordinates of the points within the envelope polygon with an elevation higher or equal to the 95th percentile of the elevation of all envelope points.

The inventories only contain entries for locations with actual landslides and therefore a sufficient soil thickness. To better reflect the fact that landslides cannot occur in areas with bare rock, additional points with a landslide thickness of 0 m in rocky areas were added to the analysis dataset (step S2.2 in Fig. 3). The points were randomly generated within the areas marked as rock or loose rock in the ground cover layer of the swissTLM3D landscape model (Swisstopo, 2023b). The points were generated separately for each dataset and only for the rock signatures within the catchments that contain slide events. The number of generated points is proportional to the percentage of the catchments covered by the rock signature, namely 34 points for the HMDB dataset (4.1% rock cover) and 53 points (9.7% rock cover) for the KtBE Dataset.

4.3 Modelling and analysis

4.3.1 Models and covariate selection

We tested three different types of ML models for predicting the potential failure thickness of shallow landslides. The R caret package (Classification And REgression Training) (Kuhn, 2008) was used to fit these models. Due to the promising performance of random forests (hereafter RF) in other studies, our development efforts were mainly focused on RF models (Breiman, 2001) implemented using the ranger package (Wright and Ziegler, 2017). In addition, generalized additive models (hereafter GAM) via the mgcv package (Wood, 2011) and linear regression (hereafter LM) using the built-in lm function of R were tested.

All three model types were trained using the same input data and validation procedures. The covariates included in the models were chosen based on a combination of exploratory analysis as well as input from literature and experts on landslides and geomorphology (step S3.1 in Fig. 3). The exploratory analysis included test-fitting RF models with both datasets to determine variable importances and attempts at automatic variable selection using recursive feature elimination. Based on these inputs, the following covariates were chosen:

- **tri_r5_5** and **tri_r5_10**: terrain ruggedness index with a radius of 5 cells for 5 m and 10 m cell sizes
- **vrm_r5_25**: vector ruggedness measure with a radius of 5 cells at 25 m cell size
- **tpi_500m_25** and **tpi_4km_25**: topographic position indexes 500 m and 4 km window size at 25 m cell size
- **vhm_max_5**: maximum vegetation height at 5 m cell size
- **h_5**: altitude above sea level sampled at 5 m cell size
- **mrvbf_10**: multiresolution index of valley bottom flatness at 10 m cell size
- **mrrtf_25**: multiresolution index of the ridge top flatness at 25 m cell size
- **slope_height_25**, **standardized_height_25**, and **valley_depth_25**: slope height, standardized height, and valley depth at 25 m cell size calculated by the SAGA module "Relative Heights and Slope Positions" (Böhner and Selige, 2006)
- **slope_10**: slope gradient in degrees at 10 m cell size

https://doi.org/10.5194/nhess-2024-76
Preprint. Discussion started: 22 May 2024


Natural Hazards and Earth System Sciences Discussions

- **aspect_nness_10**: northness of the aspect calculated as cosine(aspect) at 10 m cell size
- **twi_5**, **catchment_area_25**, and **catchment_slope_25**: topographic wetness index, catchment area and catchment slope at 5 m and 25 m cell size as calculated by the SAGA module "SAGA Wetness Index" (Böhner et al., 2002; Böhner and Selige, 2006)
- **curvature_10** and **curvature_profile_25**: general curvature at 10 m cell size and profile curvature at 25 cell size as calculated by the SAGA module "Slope, Aspect, Curvature"
- **openness_neg_200_5**: negative openness calculated with a radius of 200 m at 5 m cell size
- **rhob_m**: mean bulk density of the local lithology

To enable additional comparisons, three existing models for predicting soil depth were applied in addition to the three ML models. The models were chosen for comparison because the soil thickness is closely related to the thickness of landslides and, therefore, is often used as a proxy for landslide thickness. The first two existing models that we adapted were proposed by Saulnier et al. (1997). They use a predicted soil depth based on either elevation (hereafter Simple-Z) or slope (hereafter Simple-S) by applying a linear interpolation based on the minimum and maximum values in a set of reference data. The third method used for comparison, proposed by van Zadelhoff et al. (2022) (hereafter SFM), also uses the slope to predict soil depth. However, to account for the shallow soils on steep slopes the method derives the soil thickness from a log-normal distribution and multiplies it by a correction factor which is a function of the slope inclination. For the Simple-Z model, the elevation sampled at 5 m cell size was used to train the model. For the Simple-S and the SFM model, the slope sampled at 10 m cell size was used since it showed the best fit with the slopes at the failure point recorded in the inventories.

4.3.2 Training and validation

Separate models were trained for the HMDB and KtBE datasets, resulting in 12 models overall (step S3.2 in Fig. 3). Both datasets were each split into training data (80%) and validation data (20%). All models were trained using 10-fold cross validation (James et al., 2021). The built-in caret functions were used for the RF, GAM and LM models, and custom cross validation methods were written for the Simple-Z, Simple-S and SFM models. Since the hyper-parameters of an RF model can significantly influence model performance (Huang and Boutros, 2016; Probst et al., 2019), the training of the RF model was combined with a hyper-parameter tuning leveraging a modified version of the tune-grid functionality included in the caret package. The function performs a grid search over the parameters and values shown in Tab. 4. Similarly, the standard hyper-parameters for GAM and LM available in caret are tuned. The final RF models for both datasets used the splitrule "maxstat", a minimum node size of 2, and 22 variables to split on. The HMDB-trained model used 100 trees with a maximum depth of 150 while the KtBE-trained model used 50 trees with a maximum depth of 50. For the GAM models of both datasets, the "REML" method was used for smoothing parameter estimation. The KtBE-trained model was fitted with possible penalisation of terms while the HMDB-trained model was fitted without. For the LM model, both the HMDB-trained and the KtBE-trained models were fit without intercept.

https://doi.org/10.5194/nhess-2024-76
Preprint. Discussion started: 22 May 2024

Natural Hazards and Earth System Sciences
Discussions

Table 4. Parameters and values for tuning the hyper-parameters for the random forests (RF), generalized additive model (GAM) and linear regression (LM) models.

Model	Parameter	Default value	Values
RF	Number of variables considered to split at each node	Square root of the number of variables	2, 6, 8, 10, 22
	Splitting rule	'variance'	'variance', 'extratrees', 'maxstat'
	Minimal node size to split at	5 (for regressions)	2, 6, 8, 10, 12
	Number of trees	500	50, 100, 200
	Maximal tree depth	unlimited	50, 100, 150, 200, 250
GAM	Smoothing parameter estimation method	Generalized Cross Validation (GCV) with Mallows' Cp for scale	'GCV.Cp', 'REML'
	Possible removal of terms through penalisation	FALSE	TRUE, FALSE
LM	Whether to fit with or without intercept	Fit with intercept	TRUE, FALSE

Performance measures were calculated based on the application of the trained models to the respective validation data in order to assess model performance (step S3.3 in Fig. 3). In addition, the models trained with the HMDB dataset were cross-applied to the KtBE validation data and vice versa to evaluate the transferability across datasets. The mean absolute error (MAE) of the landslide thickness and the R^2 value were used as measures of the model performance.

We used the mean absolute error (MAE) of predicted landslide thickness versus landslide thickness from the inventory as the primary performance assessment measure, which was calculated as:

$$MAE = \frac{1}{n_{slides}} \Sigma_{i=1}^{n_{slides}} \left| y_{Actual_i} - y_{Predicted_i} \right| \quad \text{(Eq. 1)}$$

Where:

MAE: Mean absolute error of the landslide failure thickness
y_{Actual_i}: Landslide failure thickness in m for landslide i according to the inventory
$y_{Predicted_i}$: Landslide failure thickness in m for landslide i predicted by the model
n_{slides}: Total number of landslides in the reference data

Additionally, we calculated the coefficient of determination R^2 to judge how good the fit between the predicted and actual data is:

$$R^2 = cor(y_{Actual}, y_{Predicted})^2 \quad \text{(Eq. 2)}$$

https://doi.org/10.5194/nhess-2024-76
Preprint. Discussion started: 22 May 2024

Where:

R^2: Coefficient of determination

y_{Actual}: Landslide failure thicknesses in m according to the inventory

$y_{Predicted}$: Landslide failure thickness in m predicted by the model

5 Results

5.1 Statistical properties of landslide inventories

The distributions of the landslide thickness in the HMDB and KtBE datasets are very similar, with an identical mean of 0.7 m and a median of 0.6 m in the HMDB and 0.5 m in the KtBE dataset (see Tab. 5). As can be seen in Fig. 4 (a), 90% of the landslides had a thickness smaller than or equal to 1 m in the HMDB and the KtBE dataset and both show peaks at 0.5 m and 1 m. This is especially the case for the KtBE dataset, which also shows additional small peaks at 1.5 m and 2 m landslide thickness. In contrast, the thickness values for the StorMe dataset show dominant peaks at 0.5 m, 1 m, 1.5 m, and 2 m with both the median and mean at 1 m. Most of the landslides were up to 1 m thick with more than 25% of the landslides recorded at 1 m thickness. Figure 5 shows the distribution of the landslide thickness over the slope classes. The KtBE dataset shows a clear trend towards decreasing landslide thicknesses and lower variance with increasing slope steepness. The HMDB dataset, on the other hand, shows only a weak trend towards such a decrease. Because of missing slope values, the trend in the StorMe dataset can only be evaluated by the sampled slope values. StorMe also tends towards fewer landslides at higher slope values but with larger interquartile intervals for the thickness. In both the HMDB and KtBE datasets, landslides occurred at slope angles above 15°, with the trend in the number of occurrences increasing with the slope angle and a relatively sharp decrease above 40° (Fig. 4). Half of the landslides occurred above 36° in the HMDB and above 31° in the KtBE dataset. Almost no landslides occurred on slopes with more than 55° or below 15° slope angle. A visual verification of the landslides below and above these boundaries confirmed that most of the failures are plausible. The StorMe dataset does not contain sufficient recorded slope values for a reliable interpretation of the failure occurrence at specific slope values. The landslides below 15° (HMDB: n=16, KtBE: n=5) were mostly directly located at a transition between flat and steep terrain (e.g., a terrace or a road), which leads to a low mean slope angle at the failure area. The landslides with a slope angle above 55° (HMDB: n=4) were all located in forested areas, with two of them being located at a transition between steeper and less steep terrain. The comparison of the recorded slope values with those from the covariates sampled at 5 m cell size showed slightly lower mean and median values for the HMDB dataset and very similar values for the KtBE dataset. The elevation range where shallow landslides occurred, as well as its distribution, is similar in both datasets (5).

https://doi.org/10.5194/nhess-2024-76
Preprint. Discussion started: 22 May 2024

Natural Hazards and Earth System Sciences
Discussions

Table 5. Summary statistics including the total number of records (n), n within forests, the minimum, median, mean, maximum, and standard deviation (SD) for important characteristics of shallow landslides derived from the landslide inventories as well as from covariates.

Source	Variable	Dataset	n	(n in forest)	Min	Median	Mean	Max	SD
Inventory	Landslide thickness [m]	HMDB	709	(319)	0.1	0.7	0.6	2.0	0.3
		KtBE	517	(20)	0.2	0.7	0.5	2.5	0.4
		StorMe	2988	(837)	0.1	1.0	1.0	2.5	0.5
	Slope [°]	HMDB	648	(295)	1.0	35.1	36.0	80.0	9.0
		KtBE	517	(20)	8.3	31.0	31.1	52.5	5.8
		StorMe	17	(5)	20.0	35.5	35.	45.0	6.9
Covariates	Elevation [m]	HMDB	709	(319)	523	1214	1188	2257	290
		KtBE	517	(20)	624	1334	1283	2288	369
		StorMe	2988	(837)	395	1075	1036	2369	348
	Slope 5 m [°]	HMDB	709	(319)	6.0	33.3	34.3	58.9	7.8
		KtBE	517	(20)	8.2	31.3	31.8	48.3	6.6
		StorMe	2988	(837)	0.0	28.2	28.8	64.8	9.5

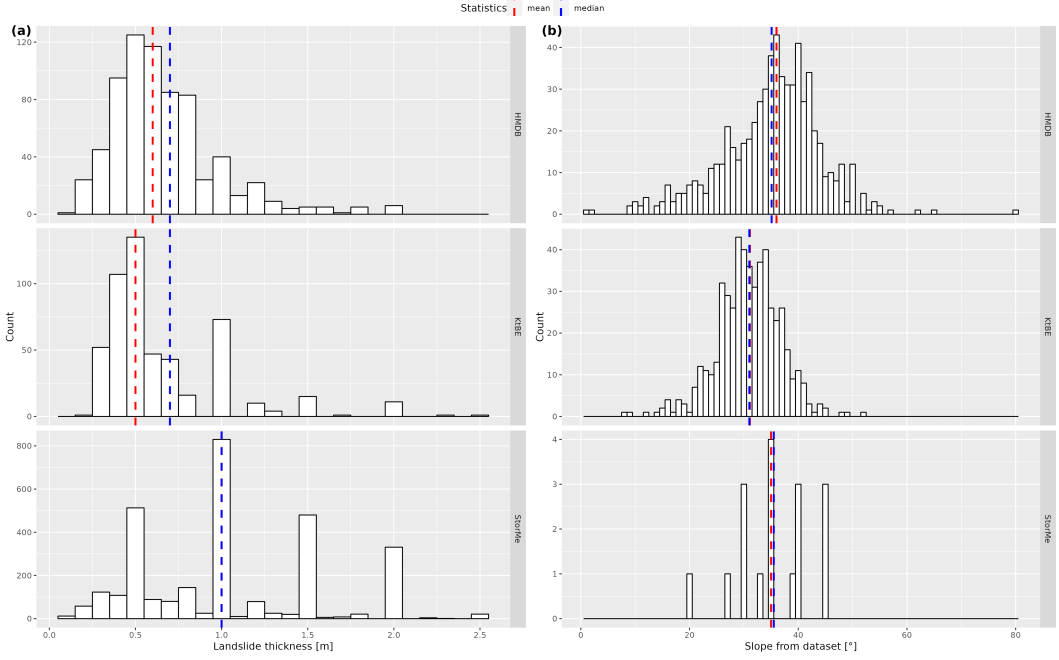

Figure 4. Histograms showing the distribution of (a) the landslide thickness and (b) the mean slope values in the release areas recorded in the three datasets.

https://doi.org/10.5194/nhess-2024-76
Preprint. Discussion started: 22 May 2024

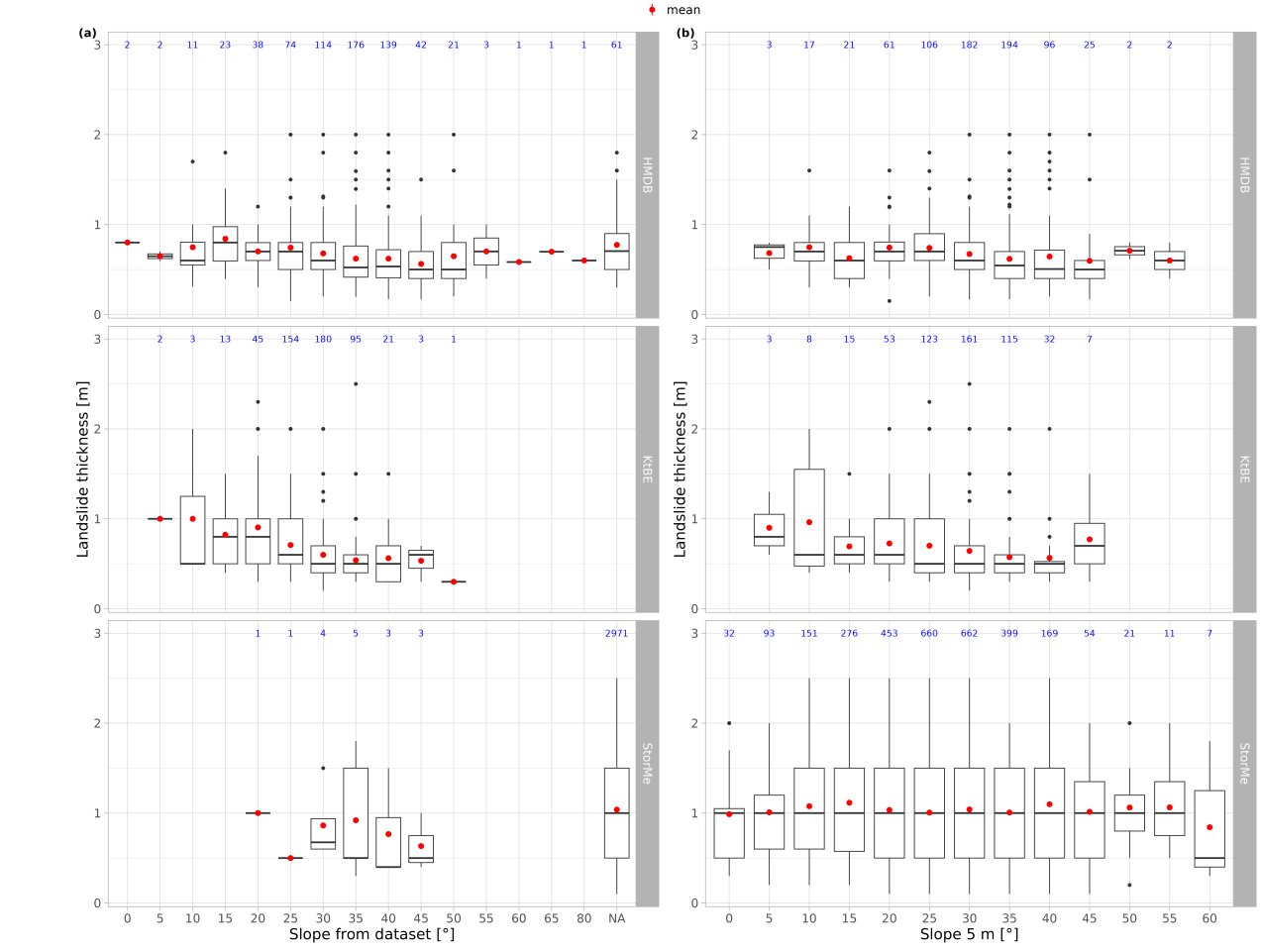

Figure 5. Box plots showing the distribution of the landslide thickness over slope classes based on (a) the reported slope for the different datasets and (b) the slope values sampled at 5 m cell size. The red dots represent the mean value while the blue numbers show the number of records per slope class.

5.2 Modelling results

Overall, the RF models performed best with an MAE of 0.24 m for the HMDB and 0.19 m for the KtBE dataset (see Tab. 6). While the MAE values of the GAM and LM models are comparable for the respective datasets, their R^2 values tend to be lower in comparison to the RF models. Furthermore, both the GAM and LM models show some outliers in the positive and negative direction with values between -0.5 m to 4.8 m for the predictions and -4.1 m to 2.1 m for the error. The Simple-Z and Simple-S models clearly showed worse performance with MAE values exceeding 1 m. The SFM model achieved MAE values of 0.37 m for HMDB and 0.36 m for KtBE. When comparing the performance between the datasets, the models for the KtBE dataset performed slightly better than the HMDB-trained models. The results for the cross-application are variable. In most

https://doi.org/10.5194/nhess-2024-76
Preprint. Discussion started: 22 May 2024

Natural Hazards and Earth System Sciences
Discussions

315 cases, MAE values were comparable to those of the model trained with the same dataset with differences between 1 cm to 10 cm for the ML models and between -36 cm and 36 cm for the existing models.

Table 6. Performance of the trained models. Results are shown for the application to the validation data of the respective dataset as well as for the cross-application to the other dataset. n_{test} denotes the number of records in the validation data. $Prediction_{min}$/$Prediction_{max}$ correspond to the minimum/maximum predicted values while $Error_{min}$/$Error_{max}$ correspond to the minimum/maximum error. AE_{p90} denotes the 90th percentile of the absolute error.

Model type	Training dataset	Validation dataset	n_{test}	MAE	R^2	$Prediction_{min}$	$Prediction_{max}$	$Error_{min}$	$Error_{max}$	AE_{p90}
Random Forest	HMDB	HMDB	138	0.25	0.11	0.12	0.85	-0.53	1.35	0.54
Random Forest	BE	BE	112	0.19	0.44	0.01	1.10	-0.54	1.73	0.39
Random Forest	BE	HMDB	743	0.26	0.07	0.00	1.25	-0.73	1.64	0.56
Random Forest	HMDB	BE	570	0.28	0.17	0.05	0.86	-0.66	1.90	0.49
GAM	HMDB	HMDB	138	0.25	0.09	0.08	0.79	-0.48	1.49	0.50
GAM	BE	BE	112	0.20	0.34	-0.18	1.17	-0.42	2.05	0.39
GAM	BE	HMDB	743	0.26	0.06	-0.30	2.73	-2.05	1.60	0.57
GAM	HMDB	BE	570	0.27	0.19	-0.29	0.80	-0.64	1.98	0.42
LM	HMDB	HMDB	138	0.25	0.09	0.16	0.89	-0.41	1.51	0.49
LM	BE	BE	112	0.22	0.34	-0.28	0.98	-0.54	1.58	0.43
LM	BE	HMDB	743	0.26	0.03	-0.43	4.79	-4.09	1.68	0.51
LM	HMDB	BE	570	0.27	0.17	-0.45	0.93	-0.68	2.01	0.46
Simple-S	HMDB	HMDB	138	0.90	0.00	1.26	1.93	-1.93	0.63	1.25
Simple-S	BE	BE	112	1.37	0.13	1.46	2.27	-2.08	0.23	1.69
Simple-S	BE	HMDB	743	1.26	0.05	1.30	2.37	-2.37	0.30	1.62
Simple-S	HMDB	BE	570	1.01	0.13	1.00	1.93	-1.93	0.62	1.31
Simple-Z	HMDB	HMDB	138	0.87	0.09	0.50	2.01	-1.46	0.42	1.31
Simple-Z	BE	BE	112	1.11	0.18	0.14	2.24	-1.73	0.66	1.58
Simple-Z	BE	HMDB	743	1.17	0.08	0.02	2.38	-2.05	0.48	1.59
Simple-Z	HMDB	BE	570	0.87	0.15	-0.02	1.98	-1.46	0.94	1.31
SFM	HMDB	HMDB	138	0.37	0.00	0.01	1.43	-0.92	1.79	0.73
SFM	BE	BE	112	0.36	0.02	0.00	1.55	-1.24	1.75	0.81
SFM	BE	HMDB	743	0.36	0.01	0.00	1.64	-1.10	1.99	0.74
SFM	HMDB	BE	570	0.35	0.04	0.00	1.71	-1.13	1.57	0.77

The scatter plots of the actual vs. the landslide thickness predicted by the three ML models are located closer around the identity line (cf. Fig. 6). However, all three models showed a tendency to slightly overestimate lower landslide thicknesses and distinctly underestimate higher thicknesses. The Simple-S model tended to overestimate the landslide thickness clearly across
320 the whole range. The Simple-Z model showed a similar trend but with a higher variance. The SFM model also exhibited a high variance but with accurate predictions. In particular, the added points with 0 m landslide thickness showed high variances in all three of the existing models.

The distribution of the residuals per slope class (Fig. 7) was similar for most slope classes where training and validation data stem from the same dataset. Mainly the classes higher than 40° show larger interquartile intervals and higher mean values. The

https://doi.org/10.5194/nhess-2024-76
Preprint. Discussion started: 22 May 2024


Natural Hazards and Earth System Sciences
Discussions

existing models generally also had higher variances than the ML models. Looking at the cross-application of the models (see Fig. A1 in Appendix A1), there are evidently more outliers and higher variances across all slope classes. In particular, the 5° class of the KtBE-trained models applied to the HMDB data consistently showed high variances.

https://doi.org/10.5194/nhess-2024-76
Preprint. Discussion started: 22 May 2024

Natural Hazards and Earth System Sciences
Discussions
Open Access
EGU

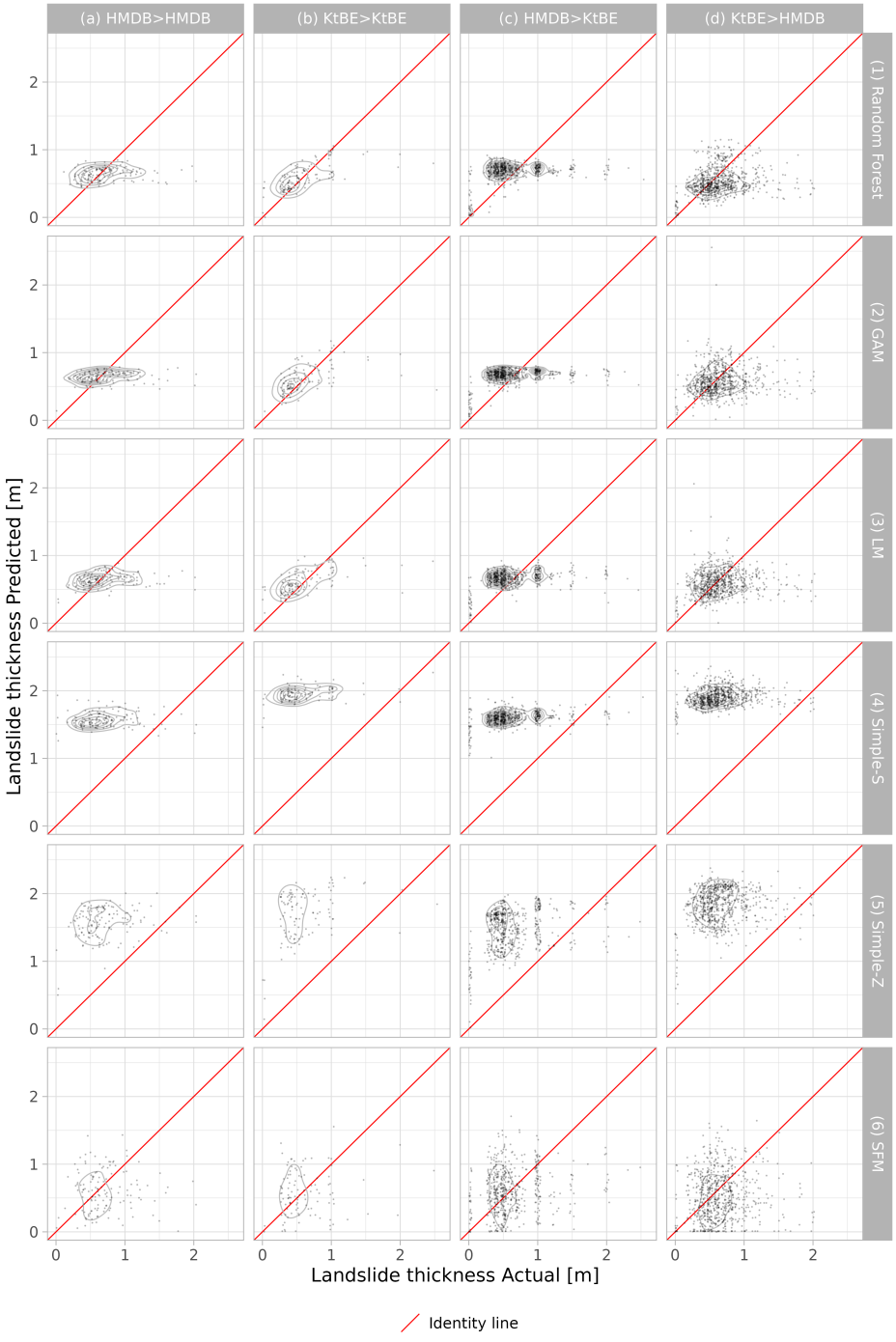

Figure 6. Scatter plots showing the actual vs. the predicted landslide thickness differentiated by model type (rows) and dataset (columns): (a) model trained and tested with HMDB dataset, (b) model trained and tested with KtBE dataset, (c) model trained with HMDB and tested with KtBE dataset, and (d) model trained with KtBE and tested with HMDB dataset. The diagrams have 2D kernel density contours in the background as well as the identity line in red. Note that some outliers for the GAM and LM models are outside the display range of the plots.

https://doi.org/10.5194/nhess-2024-76
Preprint. Discussion started: 22 May 2024

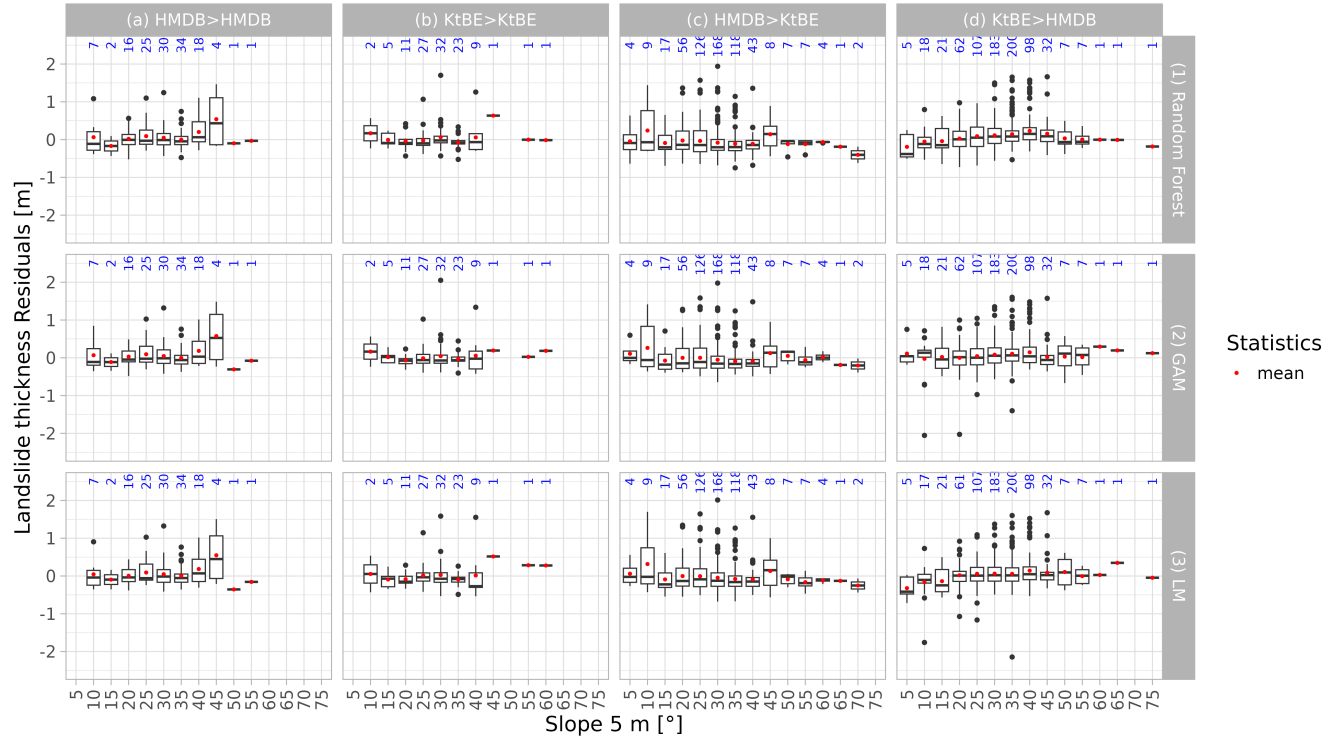

Figure 7. Box plots showing slope classes sampled at 5 m cell size vs. the residuals of the predicted landslide thickness for the best three models differentiated by model type (rows) and dataset (columns, see caption Fig. 6 for details). The red dots represent the mean value while the blue numbers show the number of entries per slope class. Note that some outliers are outside the plotted range.

Although the analysis of the variable importance of the ML models showed clear differences between the models, the variables elevation, terrain roughness index at 10 m cell size, mean density of the local lithology, negative openness, and multiresolution valley bottom flatness are found more often among the top-ranked ones. The hyper-parameter tuning resulted in a reduction of the MAE of up to 2 cm for certain models. The chosen parameters were the same across most of the datasets.

6 Discussion

6.1 Landslide inventories

The slope values recorded in the HMDB and KtBE landslide inventories largely match the ranges found in the literature, with reported values from 5° to 35° (Guzzetti et al., 2008a), from 20° to 35° (Meier et al., 2020), from 22° to 40° (Dahl et al., 2010), and from 19° to 50° (with predominant values from 25° to 45°) (Rickli and Graf, 2009) (see Fig. 4).

Larsen et al. (2010) compared data on landslide thickness from several landslide inventories (including global inventories and inventories of different locations in California, the Oregon Coast Range, and New Zealand), some of which showed peaks

https://doi.org/10.5194/nhess-2024-76
Preprint. Discussion started: 22 May 2024


Natural Hazards and Earth System Sciences
Discussions

around 0.5 m, 1 m, and 2 m similar to the ones observed in the HMDB, KtBE, and StorMe inventories. Particularly in the KtBE and StorMe datasets, the observed peaks can be attributed to estimations made during the field recording phase.

6.2 Model performance

The ML models clearly outperformed the two existing simple models based on elevation and slope proposed by Saulnier et al. (1997). However, it has to be noted that those models were originally intended to be used in smaller areas like single catchments with more uniform terrain, whereas our application covers a much larger area in Switzerland with more diverse terrain conditions. Although the SFM model proposed by van Zadelhoff et al. (2022), which was calibrated with the values from the inventories, produced better results, the RF model still yielded MAE values that were at least 17% and up to 47% lower. While the ML models exhibited low errors, they all tended to underestimate higher landslide thickness values. We attribute this to the low number of records with a landslide thickness of more than one meter in the datasets used for model training. The cross-application of the ML models showed that they are mostly transferable between the HMDB and KtBE datasets. One limiting factor may be the missing events in forests or in intensively cultivated areas not recorded in the KtBE inventory. Nevertheless, there appears to be enough similarity in the distributions of the landslide thickness over the slope classes and the covariates in both datasets to conclude that the models are transferable. This is supported by an additional test with a cross-application of the HMDB-trained model to the StorMe dataset, which showed a clear decline in performance. We attribute this mainly to the distinctly different distribution of the landslide thickness in the StorMe inventory with the dominant peaks at 0.5 m, 1 m, and 2 m. This indicates a limited generalizability of the models, albeit this may also be due to differences in data quality. It is likely that landslide thicknesses in the StorMe database were mainly recorded in distinct classes and not with actually measured values. Although comparability is limited, due to differences in the study area extents and the target variable (soil depth instead of landslide thickness), our results show similar trends as comparable studies. Catani et al. (2010) applied two existing models based on elevation and slope proposed by Saulnier et al. (1997) along with the geomorphology-based GIST model in the Terzona catchment (24 km^2) in Italy. The Simple-Z and Simple-S models performed worst with MAE values of 0.94 m and 0.54 m, while the GIST model had an MAE of 0.11 m. Subsequently, Segoni et al. (2012) applied the same models in the Armea catchment (37 km^2) in Italy where the Simple-Z and Simple-S models again performed worse with MAE values of 0.78 m and 1.03 m compared to an MAE of 0.23 m for the GIST model; an additional model linking the soil depth to the slope using an exponential function performed better with an MAE of 0.45 m. Xiao et al. (2023) applied the GIST model and the random forests-based GIST-RF model to generate soil depth maps in a section along the Yangtze River in Wanzhou County (27 km^2), where soil depth ranges from 0 m to 40 m. The MAE values of 10.6 m for the GIST showed that the original model cannot deal with the complex geological settings and high variability in soil depth at the study site. However, the GIST-RF model showed an MAE of 3.52m, demonstrating the potential for improvement through ML techniques.

The results of the ML models are promising. However, additional tests and optimisation may be advisable. In particular, we would expect the inclusion of additional records with a landslide thickness between 1 m and 2.5m to improve the model performance. The hyper-parameter tuning only yielded improvements that, overall, did not exceed a reduction of the MAE by 2 cm. However, the difference of up to 4 cm between some of the hyper-parameter combinations for the RF models shows

https://doi.org/10.5194/nhess-2024-76
Preprint. Discussion started: 22 May 2024


Natural Hazards and Earth System Sciences
Discussions

that hyper-parameter tuning is overall worthwhile. The results of the hyper-parameter tuning for the RF models also showed trends that are mostly in line with the findings reported by Probst et al. (2019). Additional model variants with and without additional points with 0 m landslide thickness in rock signature have been explored. However, while the addition of the points did lower the overall MAE of the machine learning models by about 2 cm, some of the R^2 values were slightly lowered. Given the large variance of the predictions for the 0 m thickness points, it is still not clear to us whether the addition of the points is recommendable. The scheme used for random sampling in space could potentially introduce a bias and class overlap, which may be mitigated by adopting a uniform sampling approach (Da Re et al., 2023).

6.3 Covariate selection

The selected covariates in the ML models mostly describe the terrain and its geomorphology. This shows parallels to models aiming to predict soil depth in general based on geomorphology (Catani et al., 2010; Xiao et al., 2023). There is also a notable overlap with variables that Zweifel et al. (2021) identified as important causal factors of shallow landslides in grassland regions of Switzerland. In addition, the inclusion of the lithology by proxy of the mean local density of the underlying bedrock and the inclusion of the vegetation (especially the forest) through the maximum of the VHM is also worth mentioning. While the importance of lithology varied significantly between the different model types and dataset combinations, the VHM consistently showed a higher importance for the models trained with the HMDB data compared to the KtBE-trained models. This may be due to the low number of landslides within the forest present in the KtBE data.

A variant of the ML models with the rainfall amount for a duration of 60 minutes for an extreme point precipitation event with a 10-year return period included as an additional variable was explored. The results, however, were almost identical to the model without this additional variable. We speculated *a priori* that this variable might be related to soil thickness due to an erosion effect, but this is apparently not the case or not detectable. Aiming for a model with less complexity, we finally opted to exclude this variable.

7 Conclusions

In this study, we presented an ML-based approach to predict the potential thickness of shallow landslides. The new machine learning models consistently performed at least 17% better when comparing the MAE to the previously existing models based on slope and elevation. We conclude that the selected set of covariates, including metrics on terrain, geomorphology, vegetation, and lithology, is a suitable basis for predicting shallow landslide thickness using ML. Considering the overall performance and the lack of outliers in the predictions, we consider the RF model to be the most accurate approach to generate improved inputs for slope stability models. For future work, we plan to adapt this study's RF model, which is built for predictions on single sample points, for the generation of rasters covering entire simulation extents. Further tests and refinements of the model are planned, especially by improving the input dataset with additional field data, by testing variants with additional sample points and sampling schemes for locations with 0 m landslide thickness, and by further refining the selection of covariates.

https://doi.org/10.5194/nhess-2024-76
Preprint. Discussion started: 22 May 2024

Natural Hazards and Earth System Sciences
Discussions
Open Access
EGU

Code availability. The code for this study is available on Zenodo (Schaller, 2024)

https://doi.org/10.5194/nhess-2024-76
Preprint. Discussion started: 22 May 2024

Natural Hazards and Earth System Sciences
Discussions

405 **Appendix A: Supplementary material**

A1 Detail results

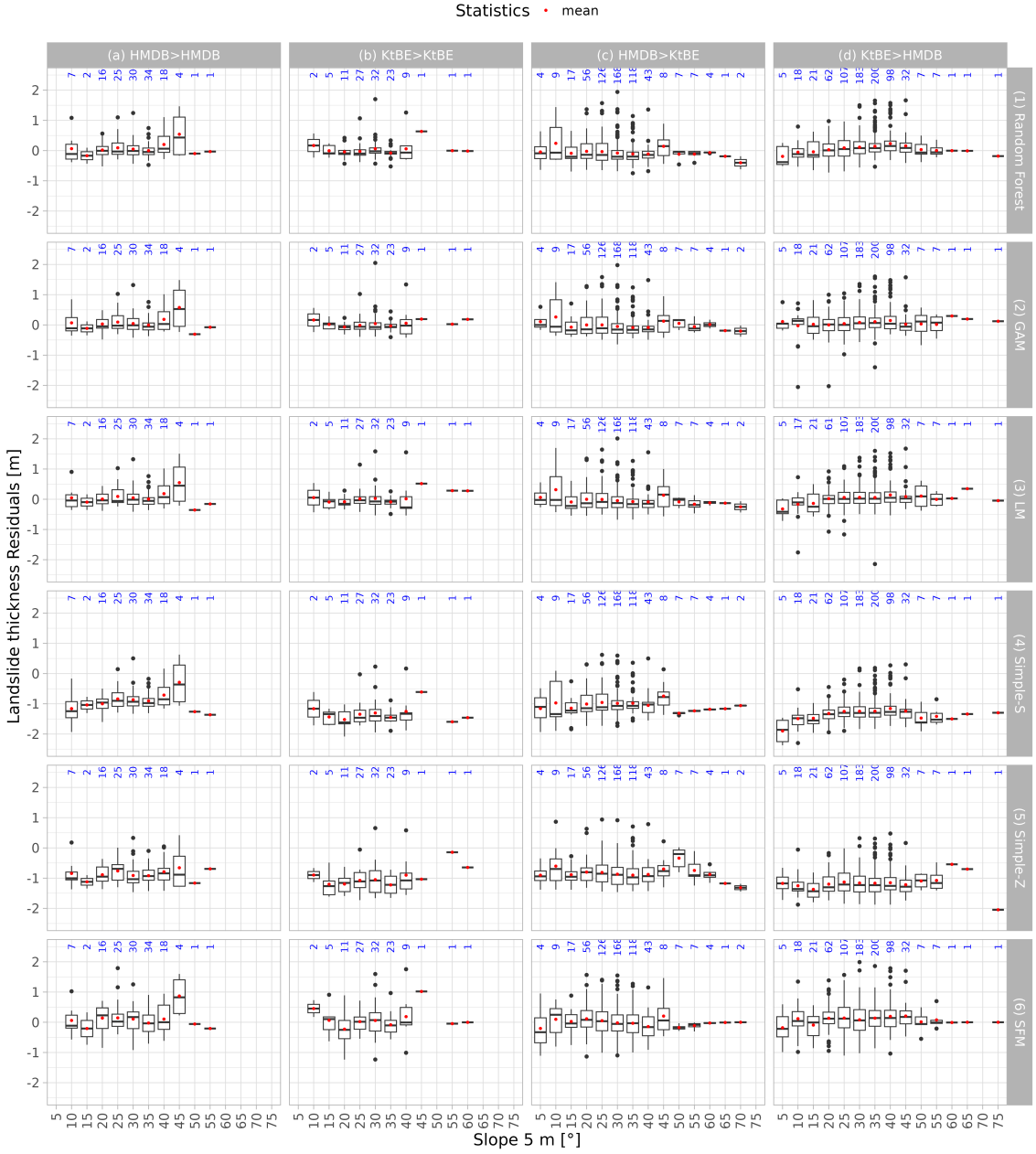

Figure A1. Box plots showing slope classes sampled at 5 m cell size vs. the residuals of the predicted landslide thickness for all models differentiated by model type (rows) and dataset (columns): (a) model trained and tested with HMDB dataset, (b) model trained and tested with KtBE dataset, (c) model trained with HMDB and tested with KtBE dataset, and (d) model trained with KtBE and tested with HMDB dataset. The red dots represent the mean value while the blue numbers show the number of entries per slope class.

https://doi.org/10.5194/nhess-2024-76
Preprint. Discussion started: 22 May 2024

Natural Hazards and Earth System Sciences
Discussions

A1 Variable importance and model tuning

Figure B1 shows the variable importance for the ML-based models. The importance values of the RF and LM were extracted from the overall result of the 10-fold cross validation result. Since no meaningful overall values could be extracted from the GAM fit, the importance values from the best model were extracted. The figure shows that there are differences in the importance of the individual variables depending on the dataset and the model. Nevertheless, several variables are more often among the top-ranked variables including the elevation, the terrain roughness index at 10 m cell size, the mean density of the local lithology, the negative openness, and the multiresolution valley bottom flatness.

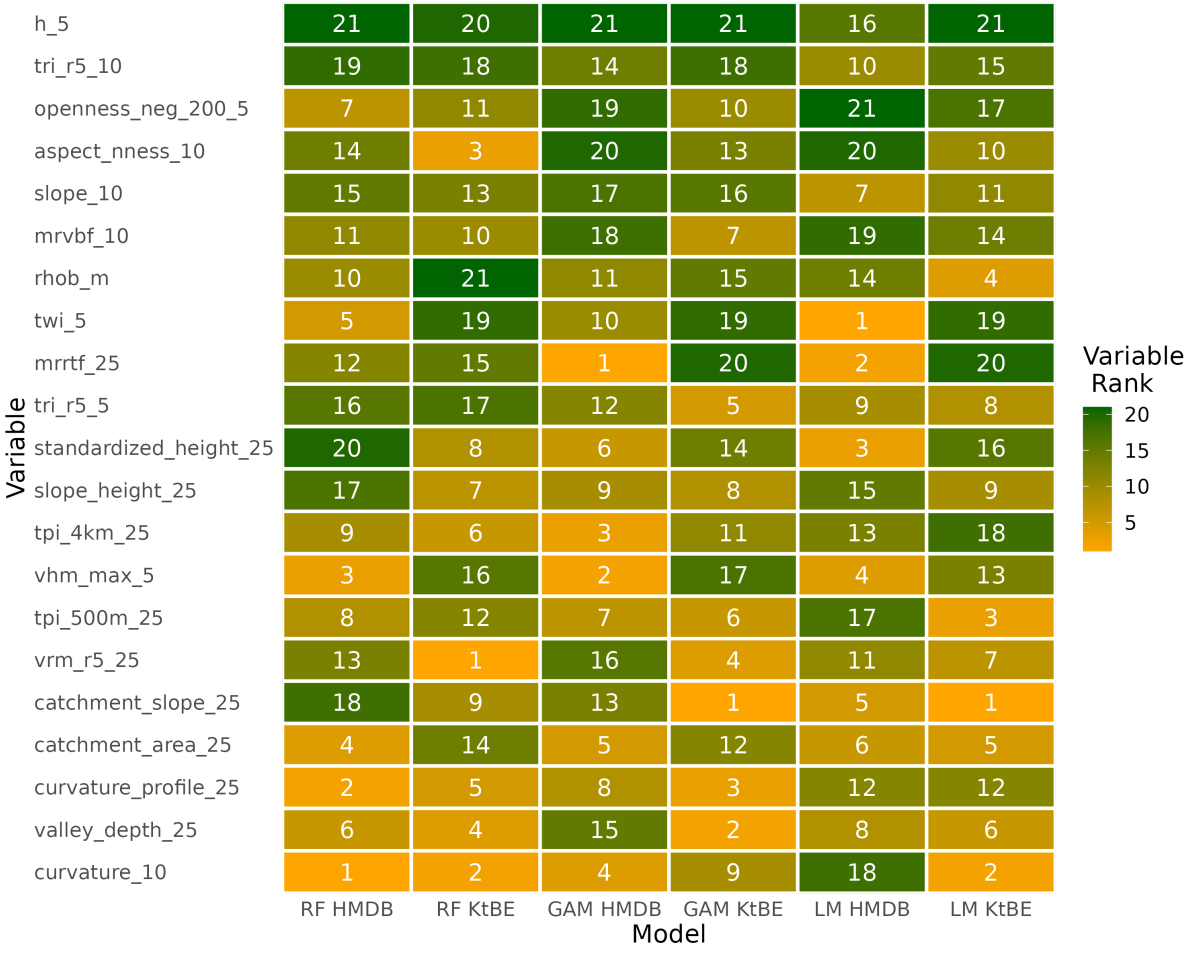

Figure B1. Heatmap showing the overall variable importance extracted from 10-fold cross validation for the RF and LM models and the importance of the best fit for the GAM model. The number in the cells and their colour correspond to the importance rank of the variable within the model, with 21 (green) being the most important and 1 (yellow) being the least important variable. The variables are sorted by the sum of the ranks of each row.

https://doi.org/10.5194/nhess-2024-76
Preprint. Discussion started: 22 May 2024

Author contributions. **Christoph Schaller:** Conceptualisation, Methodology, Software, Validation, Formal analysis, Investigation, Resources, Data Curation, Writing - Original Draft, Writing - Review & Editing, Visualisation. **Massimiliano Schwarz:** Conceptualisation, Methodology, Software, Writing - Original Draft, Writing - Review & Editing, Supervision. **Christine Moos:** Methodology, Writing - Review & Editing. **Arie C. Seijmonsbergen:** Writing - Review & Editing, Supervision. **Luuk Dorren:** Conceptualisation, Methodology, Software, Writing - Original Draft, Writing - Review & Editing, Supervision, Project administration, Funding acquisition. **Emiel van Loon:** Methodology, Writing - Review & Editing, Supervision.

Competing interests. The authors declare that they have no conflict of interest.

Acknowledgements. **Appendix C: Funding**

This work was partially funded by the Bern University of Applied Sciences and the Principality of Liechtenstein.

https://doi.org/10.5194/nhess-2024-76
Preprint. Discussion started: 22 May 2024

References

Ali, A., Huang, J., Lyamin, A. V., Sloan, S. W., Griffiths, D. V., Cassidy, M. J., and Li, J. H.: Simplified quantitative risk assessment of rainfall-induced landslides modelled by infinite slopes, Eng. Geol., 179, 102–116, https://doi.org/10.1016/j.enggeo.2014.06.024, 2014.

Arnold, P. and Dorren, L.: The Importance of Rockfall and Landslide Risks on Swiss National Roads, in: Engineering Geology for Society and Territory - Volume 6, edited by Lollino, G., Giordan, D., Thuro, K., Carranza-Torres, C., Wu, F., Marinos, P., and Delgado, C., pp. 671–675, Springer International Publishing, Cham, ISBN 978-3-319-09060-3, https://doi.org/10.1007/978-3-319-09060-3_120, 2015.

Badoux, A., Andres, N., Techel, F., and Hegg, C.: Natural hazard fatalities in Switzerland from 1946 to 2015, Nat. Hazard Earth Sys., 16, 2747–2768, https://doi.org/10.5194/nhess-16-2747-2016, publisher: Copernicus GmbH, 2016.

BAFU: Topographische Einzugsgebiete Schweizer Gewässer Schweiz, Ausgabe 2019, https://data.geo.admin.ch/ch.bafu.wasser-teileinzugsgebiete_2/, 2019.

Baum, R. L., Savage, W. Z., and Godt, J. W.: TRIGRS - a Fortran program for transient rainfall infiltration and grid-based regional slope-stability analysis, Open-File Report, https://doi.org/10.3133/ofr02424, number: 2002-424, 2002.

Bezzola, G. R. and Hegg, C.: Ereignisanalyse Hochwasser 2005, Teil 1–Prozesse, Schäden und erste Einordnung, in: Umwelt-Wissen, vol. 707, p. 215, Bundesamt für Umwelt BAFU; Eidgenössische Forschungsanstalt WSL, Bern; Birmensdorf, https://www.bafu.admin.ch/dam/bafu/de/dokumente/naturgefahren/uw-umwelt-wissen/ereignisanalyse_hochwasser2005teil1prozesseschaedenundersteeinor.pdf.download.pdf, 2007.

Breiman, L.: Random Forests, Mach. Learn., 45, 5–32, https://doi.org/10.1023/A:1010933404324, 2001.

Brenning, A.: Statistical geocomputing combining R and SAGA: The example of landslide susceptibility analysis with generalized additive models, in: SAGA – Seconds Out (= Hamburger Beitraege zur Physischen Geographie und Landschaftsoekologie, vol. 19), pp. 23–32, J. Boehner, T. Blaschke, L. Montanarella, https://fiona.uni-hamburg.de/e2bfe5e6/boehner-et-al--saga-seconds-out.pdf, 2008.

Burren, S. and Eyer, W.: StorMe–Ein informatikgestützter Ereigniskataster der Schweiz, Internationales Symposion, Interpraevent, pp. 25–35, 2000.

Böhner, J. and Selige, T.: Spatial prediction of soil attributes using terrain analysis and climate regionalisation, SAGA-Analyses and modelling applications, 115, 13–27, http://downloads.sourceforge.net/saga-gis/gga115_02.pdf, 2006.

Böhner, J., Koethe, R., Conrad, O., Gross, J., Ringeler, A., and Selige, T.: Soil regionalisation by means of terrain analysis and process parameterisation, Soil Classification 2001, pp. 213–222, https://esdac.jrc.ec.europa.eu/ESDB_Archive/eusoils_docs/esb_rr/n07_ESBResRep07/601Bohner.pdf, 2002.

Bühlmann, A. and Ruf, W.: Erfassungshandbuch StorMe 3.0 - Leitfaden zur Erfassung von Naturereignissen, https://www.bafu.admin.ch/dam/bafu/de/dokumente/naturgefahren/fachinfo-daten/storme-erfassungsrichtlinien.pdf.download.pdf/Erfassungshandbuch%20StorMe%203.0.pdf, 2020.

Caine, N.: The Rainfall Intensity - Duration Control of Shallow Landslides and Debris Flows, Geogr. Ann. A, 62, 23–27, https://doi.org/10.1080/04353676.1980.11879996, 1980.

Catani, F., Segoni, S., and Falorni, G.: An empirical geomorphology-based approach to the spatial prediction of soil thickness at catchment scale, Water Resour. Res., 46, https://doi.org/10.1029/2008WR007450, 2010.

Chang, W.-J., Chou, S.-H., Huang, H.-P., and Chao, C.-Y.: Development and verification of coupled hydro-mechanical analysis for rainfall-induced shallow landslides, Eng. Geol., 293, 106 337, https://doi.org/10.1016/j.enggeo.2021.106337, 2021.

https://doi.org/10.5194/nhess-2024-76
Preprint. Discussion started: 22 May 2024

Chinkulkijniwat, A., Tirametatiparat, T., Supotayan, C., Yubonchit, S., Horpibulsuk, S., Salee, R., and Voottipruex, P.: Stability characteristics of shallow landslide triggered by rainfall, J. Mt. Sci., 16, 2171–2183, https://doi.org/10.1007/s11629-019-5523-7, 2019.

Cohen, D., Lehmann, P., and Or, D.: Fiber bundle model for multiscale modeling of hydromechanical triggering of shallow landslides, Water Resour. Res., 45, https://doi.org/10.1029/2009WR007889, 2009.

Conrad, O., Bechtel, B., Bock, M., Dietrich, H., Fischer, E., Gerlitz, L., Wehberg, J., Wichmann, V., and Böhner, J.: System for Automated Geoscientific Analyses (SAGA) v. 2.1.4, Geosci. Model Dev., 8, 1991–2007, https://doi.org/10.5194/gmd-8-1991-2015, 2015.

Cruden, D. and Varnes, D. J.: Landslide Types and Processes, In: Turner, A.K., Schuster, R.L. (Eds.), Landslides: investigation and mitigation. National Academy Press,Washington, D.C, 247, 36–75, 1996.

Da Re, D., Tordoni, E., Lenoir, J., Lembrechts, J. J., Vanwambeke, S. O., Rocchini, D., and Bazzichetto, M.: USE it: Uniformly sampling pseudo-absences within the environmental space for applications in habitat suitability models, Methods Ecol. Evol., 14, 2873–2887, https://doi.org/10.1111/2041-210X.14209, _eprint: https://onlinelibrary.wiley.com/doi/pdf/10.1111/2041-210X.14209, 2023.

Dahl, M.-P. J., Mortensen, L. E., Veihe, A., and Jensen, N. H.: A simple qualitative approach for mapping regional landslide susceptibility in the Faroe Islands, Nat. Hazard Earth Sys., 10, 159–170, https://doi.org/10.5194/nhess-10-159-2010, publisher: Copernicus GmbH, 2010.

Di Napoli, M., Di Martire, D., Bausilio, G., Calcaterra, D., Confuorto, P., Firpo, M., Pepe, G., and Cevasco, A.: Rainfall-Induced Shallow Landslide Detachment, Transit and Runout Susceptibility Mapping by Integrating Machine Learning Techniques and GIS-Based Approaches, Water, 13, 488, https://doi.org/10.3390/w13040488, number: 4 Publisher: Multidisciplinary Digital Publishing Institute, 2021.

Dietrich, W. E., Reiss, R., Hsu, M.-L., and Montgomery, D. R.: A process-based model for colluvial soil depth and shallow landsliding using digital elevation data, Hydrol. Process., 9, 383–400, https://doi.org/10.1002/hyp.3360090311, 1995.

D'Odorico, P. and Fagherazzi, S.: A probabilistic model of rainfall-triggered shallow landslides in hollows: A long-term analysis, Water Resour. Res., 39, https://doi.org/10.1029/2002WR001595, 2003.

Dorren, L. and Schwarz, M.: Quantifying the Stabilizing Effect of Forests on Shallow Landslide-Prone Slopes, in: Ecosystem-Based Disaster Risk Reduction and Adaptation in Practice, edited by Renaud, F. G., Sudmeier-Rieux, K., Estrella, M., and Nehren, U., Advances in Natural and Technological Hazards Research, pp. 255–270, Springer International Publishing, Cham, ISBN 978-3-319-43633-3, https://doi.org/10.1007/978-3-319-43633-3_11, 2016.

Dorren, L., Sandri, A., Raetzo, H., and Arnold, P.: Landslide risk mapping for the entire Swiss national road network, Landslide Processes: from geomorphologic mapping to dynamic modeling, Strasbourg, France, pp. 6–7, 2009.

EEA: European Digital Elevation Model (EU-DEM), http://www.eea.europa.eu/data-and-maps/data/eu-dem, 2016.

Emberson, R., Kirschbaum, D., and Stanley, T.: New global characterisation of landslide exposure, Nat. Hazard Earth Sys., 20, 3413–3424, https://doi.org/10.5194/nhess-20-3413-2020, publisher: Copernicus GmbH, 2020.

Frei, C. and Fukutome, S.: Extreme Point Precipitation, in: Data and Analysis Platform, Hydrological Atlas of Switzerland, https://hydromaps.ch/#en/8/46.830/8.190/bl_hds--precip_24h_2a$4/NULL, 2022.

Froude, M. J. and Petley, D. N.: Global fatal landslide occurrence from 2004 to 2016, Nat. Hazard Earth Sys., 18, 2161–2181, https://doi.org/10.5194/nhess-18-2161-2018, publisher: Copernicus GmbH, 2018.

GDAL/OGR contributors: GDAL/OGR Geospatial Data Abstraction software Library, https://gdal.org, 2021.

Guzzetti, F., Ardizzone, F., Cardinali, M., Galli, M., Reichenbach, P., and Rossi, M.: Distribution of landslides in the Upper Tiber River basin, central Italy, Geomorphology, 96, 105–122, https://doi.org/10.1016/j.geomorph.2007.07.015, 2008a.

Guzzetti, F., Peruccacci, S., Rossi, M., and Stark, C. P.: The rainfall intensity–duration control of shallow landslides and debris flows: an update, Landslides, 5, 3–17, https://doi.org/10.1007/s10346-007-0112-1, 2008b.

https://doi.org/10.5194/nhess-2024-76
Preprint. Discussion started: 22 May 2024

Hengl, T., Mendes de Jesus, J., Heuvelink, G. B. M., Ruiperez Gonzalez, M., Kilibarda, M., Blagotić, A., Shangguan, W., Wright, M. N., Geng, X., Bauer-Marschallinger, B., Guevara, M. A., Vargas, R., MacMillan, R. A., Batjes, N. H., Leenaars, J. G. B., Ribeiro, E., Wheeler, I., Mantel, S., and Kempen, B.: SoilGrids250m: Global gridded soil information based on machine learning, PLOS ONE, 12, 0169 748, https://doi.org/10.1371/journal.pone.0169748, 2017.

Hijmans, R. J.: terra: Spatial Data Analysis, https://rspatial.org/, 2023.

Ho, J.-Y., Lee, K. T., Chang, T.-C., Wang, Z.-Y., and Liao, Y.-H.: Influences of spatial distribution of soil thickness on shallow landslide prediction, Eng. Geol., 124, 38–46, https://doi.org/10.1016/j.enggeo.2011.09.013, 2012.

Horton, P., Jaboyedoff, M., Rudaz, B., and Zimmermann, M.: Flow-R, a model for susceptibility mapping of debris flows and other gravitational hazards at a regional scale, Nat. Hazard Earth Sys., 13, 869–885, https://doi.org/10.5194/nhess-13-869-2013, 2013.

Huang, B. F. F. and Boutros, P. C.: The parameter sensitivity of random forests, BMC Bioinformatics, 17, 331, https://doi.org/10.1186/s12859-016-1228-x, 2016.

Hungr, O., Leroueil, S., and Picarelli, L.: The Varnes classification of landslide types, an update, Landslides, 11, 167–194, https://doi.org/10.1007/s10346-013-0436-y, 2014.

Hählen, N.: Kennzahlen zu spontanen Rutschungen im Kanton Bern mit Schwerpunkt auf Alpen und Voralpen, https://www.researchgate.net/publication/368510037, 2023.

Iida, T.: A stochastic hydro-geomorphological model for shallow landsliding due to rainstorm, CATENA, 34, 293–313, https://doi.org/10.1016/S0341-8162(98)00093-9, 1999.

Iverson, R. M.: Landslide triggering by rain infiltration, Water Resour. Res., 36, 1897–1910, https://doi.org/10.1029/2000WR900090, 2000.

Jaboyedoff, M., Carrea, D., Derron, M.-H., Oppikofer, T., Penna, I. M., and Rudaz, B.: A review of methods used to estimate initial landslide failure surface depths and volumes, Eng. Geol., 267, 105 478, https://doi.org/10.1016/j.enggeo.2020.105478, 2020.

James, G., Witten, D., Hastie, T., and Tibshirani, R.: An Introduction to Statistical Learning, Springer US, New York, NY, ISBN 978-1-07-161417-4, https://doi.org/10.1007/978-1-0716-1418-1, 2021.

Jia, N., Mitani, Y., Xie, M., and Djamaluddin, I.: Shallow landslide hazard assessment using a three-dimensional deterministic model in a mountainous area, Comput. Geotech., 45, 1–10, https://doi.org/10.1016/j.compgeo.2012.04.007, 2012.

Kaur, H., Gupta, S., Parkash, S., Thapa, R., Gupta, A., and Khanal, G. C.: Evaluation of landslide susceptibility in a hill city of Sikkim Himalaya with the perspective of hybrid modelling techniques, Ann. GIS, 25, 113–132, https://doi.org/10.1080/19475683.2019.1575906, 2019.

Kuhn, M.: Building Predictive Models in R Using the caret Package, J. Stat. Softw., 28, 1–26, https://doi.org/10.18637/jss.v028.i05, 2008.

Lanni, C., Borga, M., Rigon, R., and Tarolli, P.: Modelling shallow landslide susceptibility by means of a subsurface flow path connectivity index and estimates of soil depth spatial distribution, Hydrol. Earth Ssyst. Sc., 16, 3959–3971, https://doi.org/10.5194/hess-16-3959-2012, 2012.

Larsen, I. J., Montgomery, D. R., and Korup, O.: Landslide erosion controlled by hillslope material, Nat. Geosci., 3, 247–251, https://doi.org/10.1038/ngeo776, 2010.

Lateltin, O., Haemmig, C., Raetzo, H., and Bonnard, C.: Landslide risk management in Switzerland, Landslides, 2, 313–320, https://doi.org/10.1007/s10346-005-0018-8, 2005.

Leonarduzzi, E., Molnar, P., and McArdell, B. W.: Predictive performance of rainfall thresholds for shallow landslides in Switzerland from gridded daily data, Water Resour. Res., 53, 6612–6625, https://doi.org/10.1002/2017WR021044, 2017.

https://doi.org/10.5194/nhess-2024-76
Preprint. Discussion started: 22 May 2024

Li, W. C., Lee, L. M., Cai, H., Li, H. J., Dai, F. C., and Wang, M. L.: Combined roles of saturated permeability and rainfall characteristics on surficial failure of homogeneous soil slope, Eng. Geol., 153, 105–113, https://doi.org/10.1016/j.enggeo.2012.11.017, 2013.

Li, Y. and Mo, P.: A unified landslide classification system for loess slopes: A critical review, Geomorphology, 340, 67–83, https://doi.org/10.1016/j.geomorph.2019.04.020, 2019.

McColl, S. T. and Cook, S. J.: A universal size classification system for landslides, Landslides, 21, 111–120, https://doi.org/10.1007/s10346-023-02131-6, 2024.

Meier, C., Jaboyedoff, M., Derron, M.-H., and Gerber, C.: A method to assess the probability of thickness and volume estimates of small and shallow initial landslide ruptures based on surface area, Landslides, 17, 975–982, https://doi.org/10.1007/s10346-020-01347-0, 2020.

Meisina, C. and Scarabelli, S.: A comparative analysis of terrain stability models for predicting shallow landslides in colluvial soils, Geomorphology, 87, 207–223, https://doi.org/10.1016/j.geomorph.2006.03.039, 2007.

Merghadi, A., Yunus, A. P., Dou, J., Whiteley, J., ThaiPham, B., Bui, D. T., Avtar, R., and Abderrahmane, B.: Machine learning methods for landslide susceptibility studies: A comparative overview of algorithm performance, Earth-Sci. Rev., 207, 103 225, https://doi.org/10.1016/j.earscirev.2020.103225, 2020.

Milledge, D. G., Bellugi, D., McKean, J. A., Densmore, A. L., and Dietrich, W. E.: A multidimensional stability model for predicting shallow landslide size and shape across landscapes, J. Geophys. Res.-Eearth, 119, 2481–2504, https://doi.org/10.1002/2014JF003135, 2014.

Montgomery, D. R. and Dietrich, W. E.: A physically based model for the topographic control on shallow landsliding, Water Resour. Res., 30, 1153–1171, https://doi.org/10.1029/93WR02979, 1994.

Murgia, I., Giadrossich, F., Mao, Z., Cohen, D., Capra, G. F., and Schwarz, M.: Modeling shallow landslides and root reinforcement: A review, Ecol. Eng., 181, 106 671, https://doi.org/10.1016/j.ecoleng.2022.106671, 2022.

Pack, R., Tarboton, D., and Goodwin, C.: The SINMAP approach to terrain stability mapping. Procedeengs of the 8th congress of the international association of engineering geology, Vancouver, British Columbia, Canada, pp. 21–25, 1998.

Patton, N. R., Lohse, K. A., Godsey, S. E., Crosby, B. T., and Seyfried, M. S.: Predicting soil thickness on soil mantled hillslopes, Nat. Commun., 9, 3329, https://doi.org/10.1038/s41467-018-05743-y, 2018.

Pebesma, E. and Bivand, R.: Spatial Data Science: With Applications in R, Chapman and Hall/CRC, https://doi.org/10.1201/9780429459016, 2023.

Piegari, E., Cataudella, V., Di Maio, R., Milano, L., and Nicodemi, M.: A cellular automaton for the factor of safety field in landslides modeling, Geophys. Res. Lett., 33, https://doi.org/10.1029/2005GL024759, 2006.

Planchon, O. and Darboux, F.: A fast, simple and versatile algorithm to fill the depressions of digital elevation models, CATENA, 46, 159–176, https://doi.org/10.1016/S0341-8162(01)00164-3, 2002.

Probst, P., Wright, M. N., and Boulesteix, A.-L.: Hyperparameters and tuning strategies for random forest, WIREs Data Min. Knowl., 9, e1301, https://doi.org/10.1002/widm.1301, 2019.

Ran, Q., Hong, Y., Li, W., and Gao, J.: A modelling study of rainfall-induced shallow landslide mechanisms under different rainfall characteristics, J. Hydrol., 563, 790–801, https://doi.org/10.1016/j.jhydrol.2018.06.040, 2018.

Reichenbach, P., Rossi, M., Malamud, B. D., Mihir, M., and Guzzetti, F.: A review of statistically-based landslide susceptibility models, Earth-Sci. Rev., 180, 60–91, https://doi.org/10.1016/j.earscirev.2018.03.001, 2018.

Reynard, E., Häuselmann, P., Jeannin, P.-Y., and Scapozza, C.: Geomorphological Landscapes in Switzerland, in: Landscapes and Landforms of Switzerland, edited by Reynard, E., pp. 71–80, Springer International Publishing, Cham, ISBN 978-3-030-43203-4, https://doi.org/10.1007/978-3-030-43203-4_5, 2021.

https://doi.org/10.5194/nhess-2024-76
Preprint. Discussion started: 22 May 2024

Rickli, C.: Personal communication, 2023.

Rickli, C. and Graf, F.: Effects of forests on shallow landslides - case studies in Switzerland, Forest Snow and Landscape Research, pp. 33–44, https://www.dora.lib4ri.ch/wsl/islandora/object/wsl%3A15351/, 2009.

Rickli, C., McArdell, B., Badoux, A., and Loup, B.: Database shallow landslides and hillslope debris flows, 13th congress INTERPRAEVENT 2016. 30 May to 2 June 2016. Lucerne, Switzerland. Extended abstracts "Living with natural risks", pp. 242–243, https://www.dora.lib4ri.ch/wsl/islandora/object/wsl%3A20790/, 2016.

Rickli, C., Graf, F., Bebi, P., Bast, A., Loup, B., and McArdell, B.: Schützt der Wald vor Rutschungen? Hinweise aus der WSL-Rutschungsdatenbank, Schweizerische Zeitschrift für Forstwesen, 170, 310–317, https://doi.org/10.3188/szf.2019.0310, 2019.

Saulnier, G.-M., Beven, K., and Obled, C.: Including spatially variable effective soil depths in TOPMODEL, J. Hydrol., 202, 158–172, https://doi.org/10.1016/S0022-1694(97)00059-0, 1997.

Schaller, C.: HAFL-WWI/Landslide_Thickness_Prediction: Release for Predicting shallow landslide thickness using ML v0.1.1, https://doi.org/10.5281/zenodo.11032083, 2024.

Schaller, C., Ginzler, C., van Loon, E., Moos, C., Seijmonsbergen, A. C., and Dorren, L.: Improving country-wide individual tree detection using local maxima methods based on statistically modeled forest structure information, Int. J. Appl. Eearth Obs., 123, 103 480, https://doi.org/10.1016/j.jag.2023.103480, 2023.

Schuster, R. and Wieczorek, G.: Landslide triggers and types, in: Landslides - Proceedings of the First European Conference on Landslides, Prague, Czech Republic, 24-26 June 2002, pp. 59–78, Routledge, London, ISBN 978-0-203-74919-7, https://doi.org/10.1201/9780203749197-4, 2018.

Schwarz, M., Preti, F., Giadrossich, F., Lehmann, P., and Or, D.: Quantifying the role of vegetation in slope stability: A case study in Tuscany (Italy), Ecol. Eng., 36, 285–291, https://doi.org/10.1016/j.ecoleng.2009.06.014, 2010.

Segoni, S., Rossi, G., and Catani, F.: Improving basin scale shallow landslide modelling using reliable soil thickness maps, Nat. Hazards, 61, 85–101, https://doi.org/10.1007/s11069-011-9770-3, 2012.

Shano, L., Raghuvanshi, T. K., and Meten, M.: Landslide susceptibility evaluation and hazard zonation techniques – a review, Geoenvironmental Disasters, 7, 18, https://doi.org/10.1186/s40677-020-00152-0, 2020.

Sidle, R. and Ochiai, H.: Landslides: Processes, Prediction, and Land Use, ISBN 978-0-87590-322-4, https://doi.org/10.1029/WM018, 2013.

Steger, S., Schmaltz, E., Seijmonsbergen, A. C., and Glade, T.: The Walgau: A Landscape Shaped by Landslides, in: Landscapes and Landforms of Austria, edited by Embleton-Hamann, C., pp. 237–251, Springer International Publishing, Cham, ISBN 978-3-030-92815-5, https://doi.org/10.1007/978-3-030-92815-5_15, 2022.

Swisstopo: Geologie Gesteinsdichte, https://data.geo.admin.ch/ch.swisstopo.geologie-gesteinsdichte/, 2020.

Swisstopo: swissALTI3D, https://www.swisstopo.admin.ch/de/geodata/height/alti3d.html, 2023a.

Swisstopo: swissTLM3D, https://www.swisstopo.admin.ch/en/geodata/landscape/tlm3d.html, 2023b.

Team, R. C.: R: A Language and Environment for Statistical Computing, https://www.R-project.org/, place: Vienna, Austria, 2022.

van Zadelhoff, F. B., Albaba, A., Cohen, D., Phillips, C., Schaefli, B., Dorren, L., and Schwarz, M.: Introducing SlideforMAP: a probabilistic finite slope approach for modelling shallow-landslide probability in forested situations, Nat. Hazard Earth Sys., 22, 2611–2635, https://doi.org/10.5194/nhess-22-2611-2022, 2022.

Varnes, D. J.: Slope movement types and processes, Special report, 176, 11–33, 1978.

Wadoux, A. M. J. C., Minasny, B., and McBratney, A. B.: Machine learning for digital soil mapping: Applications, challenges and suggested solutions, Earth-Sci. Rev., 210, 103 359, https://doi.org/10.1016/j.earscirev.2020.103359, 2020.

https://doi.org/10.5194/nhess-2024-76
Preprint. Discussion started: 22 May 2024

Watakabe, T. and Matsushi, Y.: Lithological controls on hydrological processes that trigger shallow landslides: Observations from granite and hornfels hillslopes in Hiroshima, Japan, CATENA, 180, 55–68, https://doi.org/10.1016/j.catena.2019.04.010, 2019.

Wood, S. N.: Fast stable restricted maximum likelihood and marginal likelihood estimation of semiparametric generalized linear models, J. Roy. Stat. Soc. B, 73, 3–36, https://doi.org/10.1111/j.1467-9868.2010.00749.x, 2011.

Wright, M. N. and Ziegler, A.: ranger: A Fast Implementation of Random Forests for High Dimensional Data in C++ and R, J. Stat. Softw., 77, 1–17, https://doi.org/10.18637/jss.v077.i01, 2017.

WSL and BAFU: Dokumentation von Hangmuren und spontanen Rutschungen, https://hangmuren.wsl.ch/static/pdf/Anleitung_HMDB_V9.pdf, 2018.

Xiao, T., Segoni, S., Liang, X., Yin, K., and Casagli, N.: Generating soil thickness maps by means of geomorphological-empirical approach and random forest algorithm in Wanzhou County, Three Gorges Reservoir, Geosci. Front., 14, 101 514, https://doi.org/10.1016/j.gsf.2022.101514, 2023.

Zappone, A. and Kissling, E.: SAPHYR: Swiss Atlas of Physical Properties of Rocks: the continental crust in a database, Swiss J. Geosci., 114, 13, https://doi.org/10.1186/s00015-021-00389-3, 2021.

Zhang, S., Xu, Q., and Zhang, Q.: Failure characteristics of gently inclined shallow landslides in Nanjiang, southwest of China, Eng. Geol., 217, 1–11, https://doi.org/10.1016/j.enggeo.2016.11.025, 2017.

Zimmermann, F., McArdell, B. W., Rickli, C., and Scheidl, C.: 2D Runout Modelling of Hillslope Debris Flows, Based on Well-Documented Events in Switzerland, Geosci., 10, 70, https://doi.org/10.3390/geosciences10020070, number: 2 Publisher: Multidisciplinary Digital Publishing Institute, 2020.

Zweifel, L., Samarin, M., Meusburger, K., and Alewell, C.: Investigating causal factors of shallow landslides in grassland regions of Switzerland, Nat. Hazard Earth Sys., 21, 3421–3437, https://doi.org/10.5194/nhess-21-3421-2021, publisher: Copernicus GmbH, 2021.